Loss of Relativistic and Ultra-Relativistic Electrons From the Radiation Belts

Yuri Shprits[1,2], Nikita Aseev[1,2],Alexander Drozdov[1], Adam Kellerman[1], Maria Usanova[4], Irina Zhelavskaya[1,2], Ingo Michaelis[2], J Sebastián Cervantes[2], Dedong Wang[2], Angelica Castillo[2]

Collaborators:

Maria Spasojevic[3], Mark Engebretson[5], Oleksiy Agapitov[6,7] , Tero Raita[8], Harlan Spence[9], Daniel Baker[4], Hui Zhu[1], Richard Horne[10]

1 Department of Earth, Planetary, and Space Sciences, University of California, Los Angeles, California, USA

2 GFZ, German Research Centre For Geosciences, Potsdam, Germany and University of Potsdam, Potsdam, Germany

3 Department of Electrical Engineering, Stanford University, Stanford, California, USA

4 Laboratory for Atmospheric and Space Physics, University of Colorado Boulder, Boulder, Colorado, USA

5 Physics Department, Augsburg College, Minneapolis, Minnesota, USA

6 Space Sciences Laboratory, University of California, Berkeley, California, USA

7 National Taras Shevchenko University of Kyiv, Kyiv, Ukraine

8 Sodankylä Geophysical Observatory, Sodankylä, Finland and University of Oulu, Oulu Finland

9 Institute for the Study of Earth Oceans and Space, University of New Hampshire, Durham, New Hampshire, USA

10 British Antarctic Survey, Cambridge, UK

Outline

- Introduction
- Radiation belt loss due to the outward radial diffusion
- Modeling evidence for the scattering loss by EMIC waves
- New evidence for the loss due to EMIC waves
- Conclusions

Analysis of Loss by EMIC waves

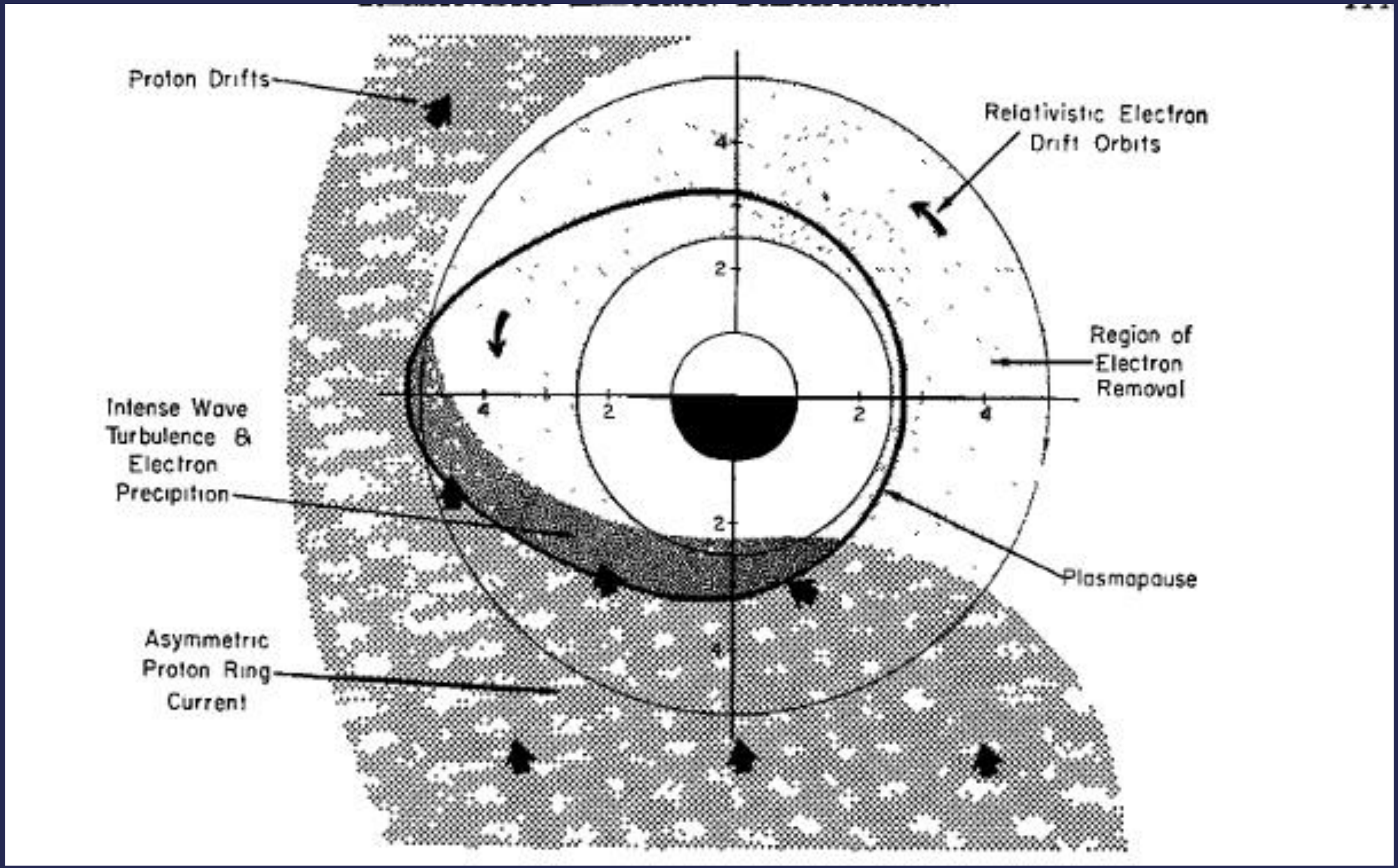

[Thorne and Kennel, 1971, *JGR*]

- Illustration of the resonant scattering of electrons by EMIC waves, that are produced by ring current protons.

- Left hand polarized EMIC waves can scatter relativistic electrons into the loss cone where they will be lost due to collisions with atmospheric particles.

Loss of Relativistic Electrons in the Radiation Belts

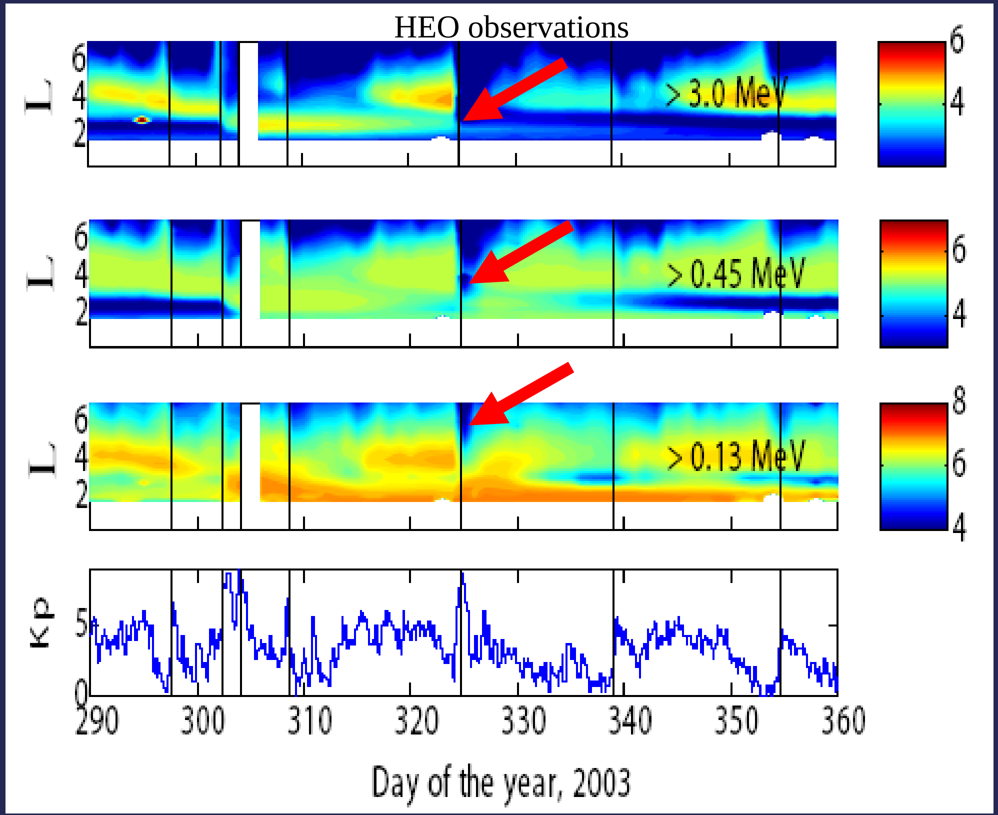

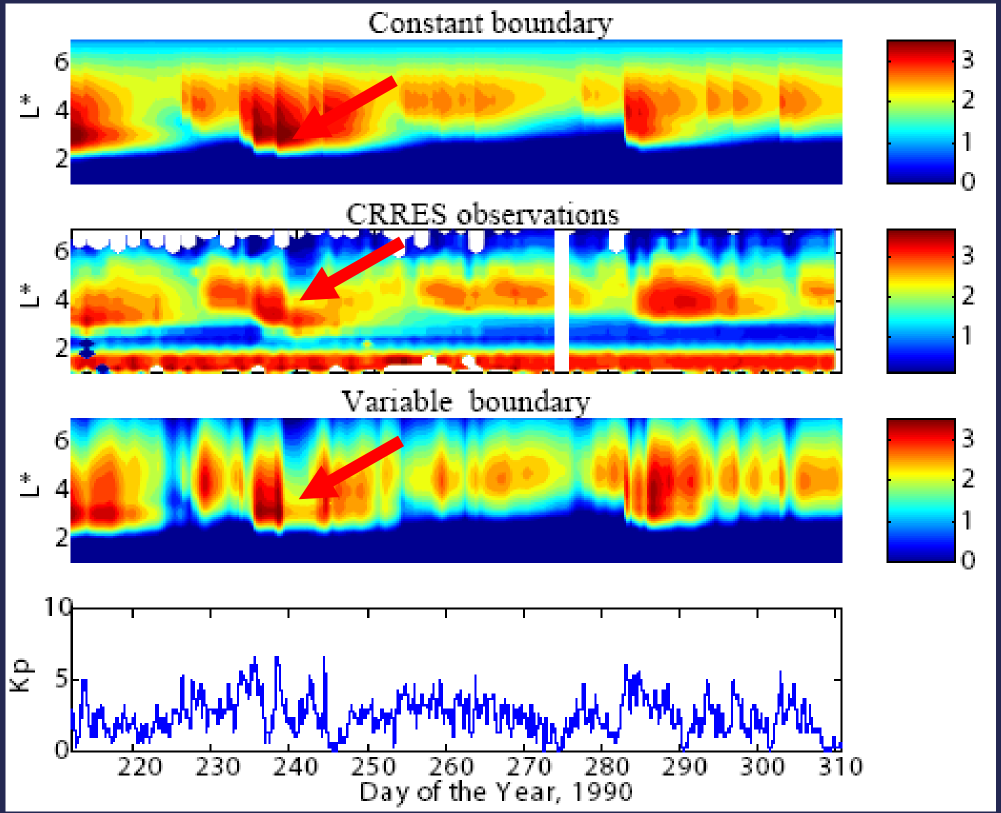

[Shprits et al., 2006, *JGR*]

Dropouts occur when the magnetosphere is compressed and occurs at low energy. The low energy dropouts cannot be explained by EMIC wave scattering. Radial diffusion simulations show that the outward radial diffusion can propagate losses down to low L-shells. Additional evidence: [Shprits et al., 2012; Ni et al., 2013; Turner et al., 2012].

Evolution of the Pitch Angle Distribution during the January 17, 2013 Storm

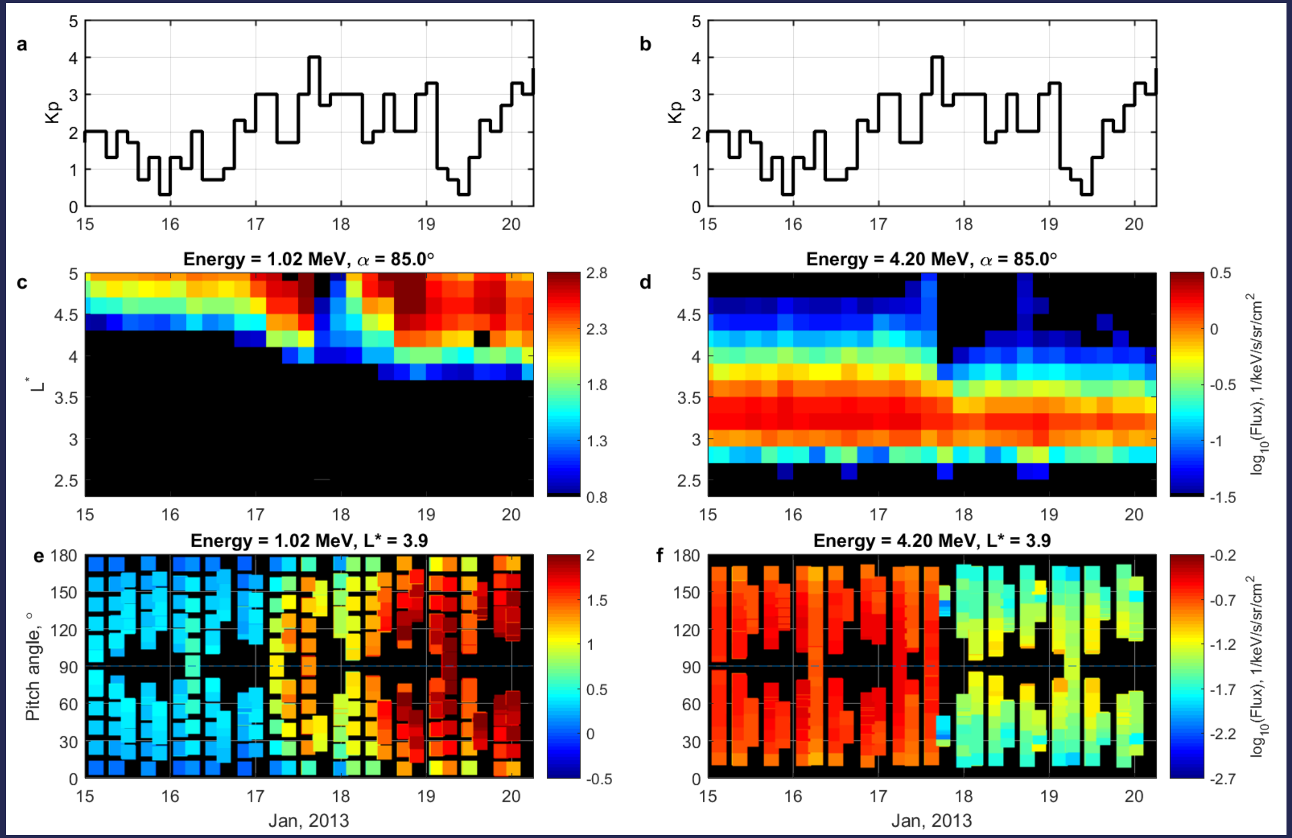

[Shprits et al., 2016, *Nature Comms*.]

Unique conditions during the January 17, 2013 storm:

1) Pre-storm peak fluxes of relativistic and ultra-relativistic electrons were separated.
2) Magnetopause was not compressed inside GEO.
3) The previous October storm created an abundance of ultra-relativistic electrons which allowed us to measure pitch-angle distributions on REPT.

Comparison of Model and Observations at Multiple Energies

- At MeV energies model can reproduce acceleration and widening of the belts.
- At Multi-MeV the model reproduces the dropout and narrowing of the pitch angle distribution.

Data

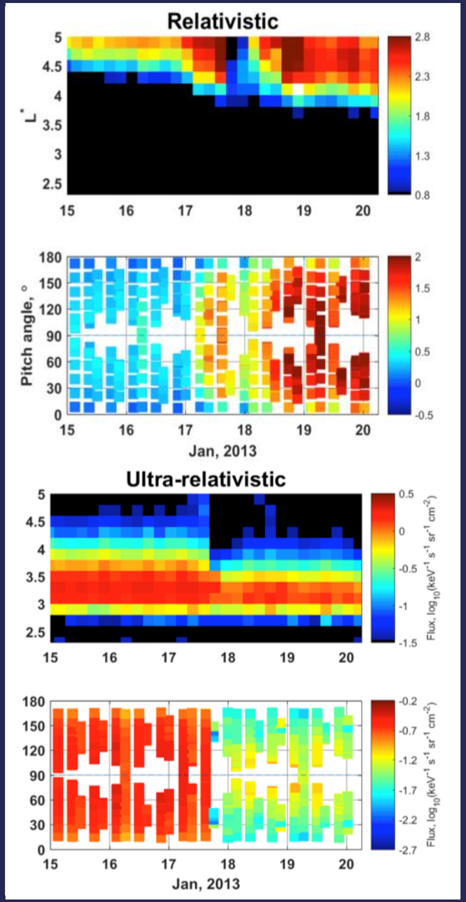

[Shprits et al., 2016, *Nature Comms.*]

Comparison of Model and Observations at Multiple Energies

- At MeV energies model can reproduce acceleration and widening of the belts.
- At Multi-MeV the model reproduces the dropout and narrowing of the pitch angle distribution.

Data **Model, no EMIC waves**

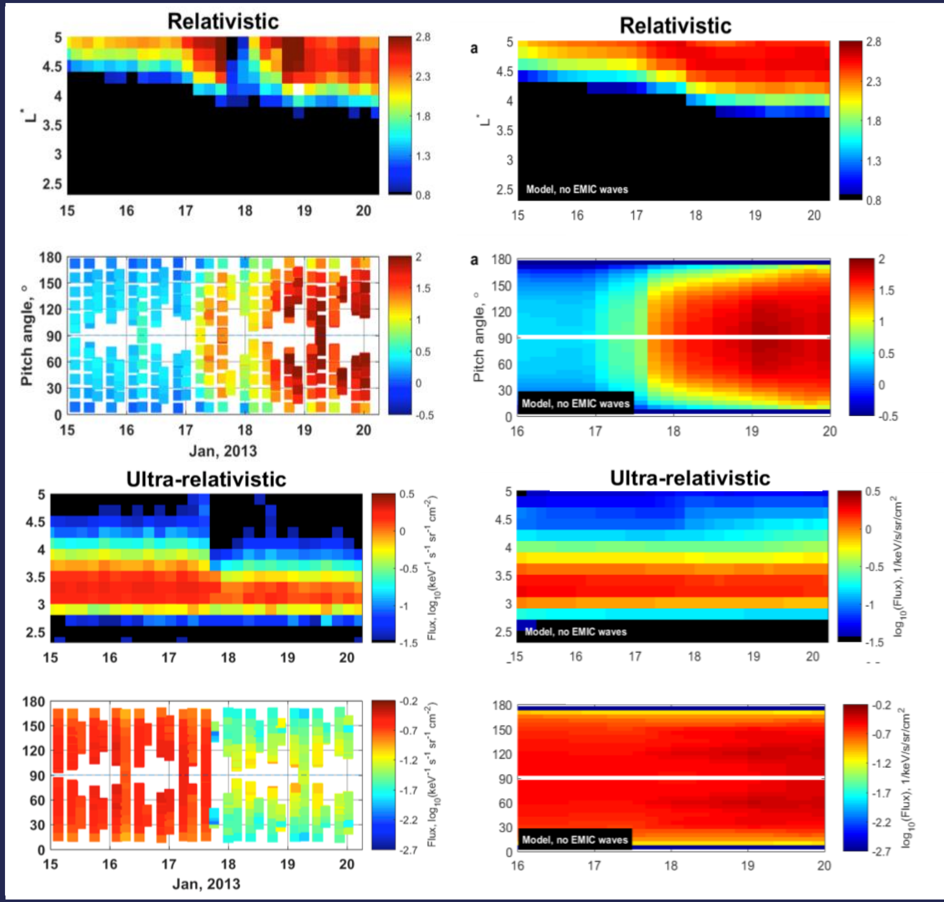

[Shprits et al., 2016, *Nature Comms.*]

Comparison of Model and Observations at Multiple Energies

- At MeV energies model can reproduce acceleration and widening of the belts.
- At Multi-MeV the model reproduces the dropout and narrowing of the pitch angle distribution.

Data | **Model, no EMIC waves** | **Model, with EMIC waves**

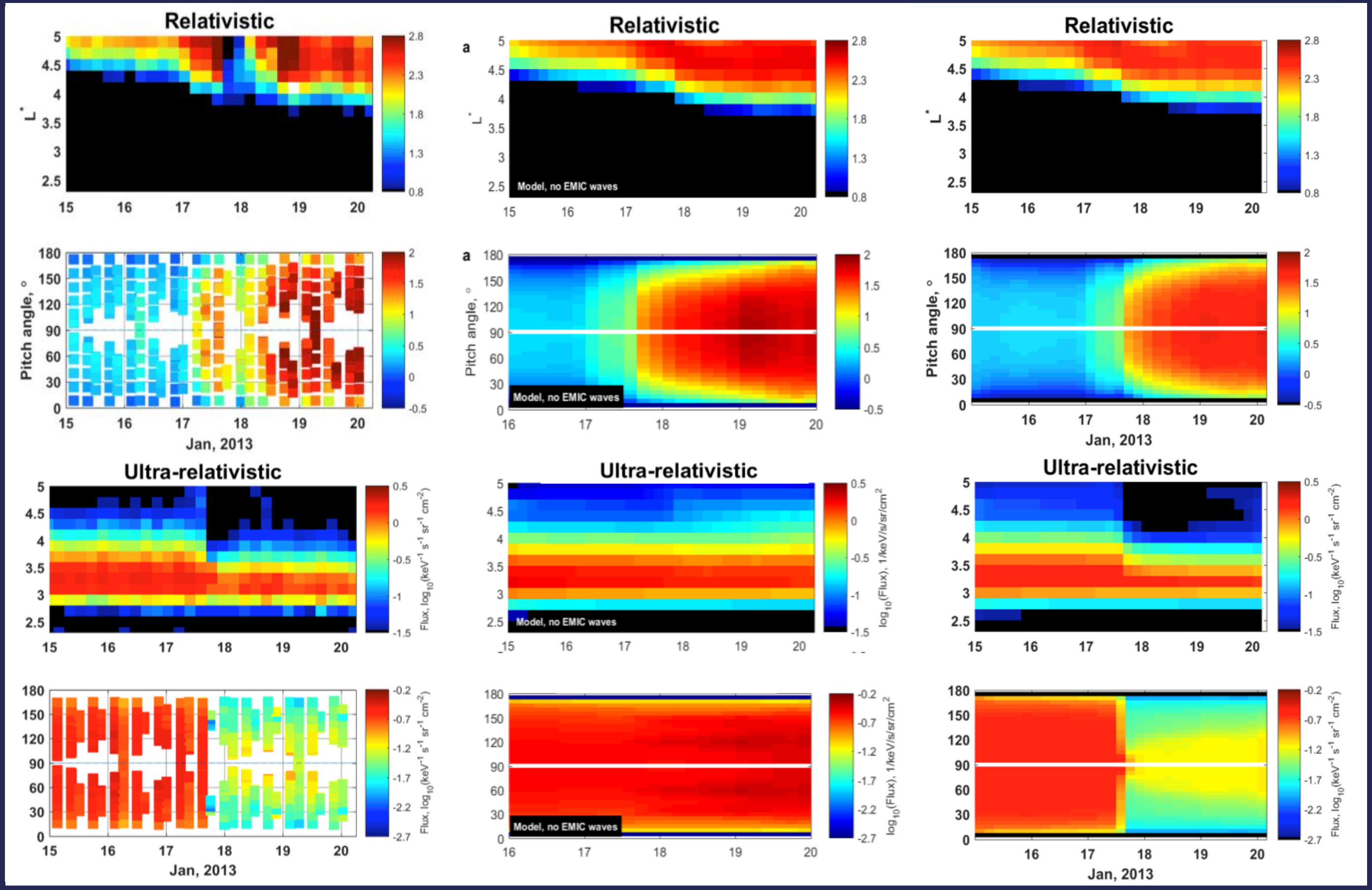

[Shprits et al., 2016, *Nature Comms.*]

Three Scenarios of the Evolution of the PSD Profiles

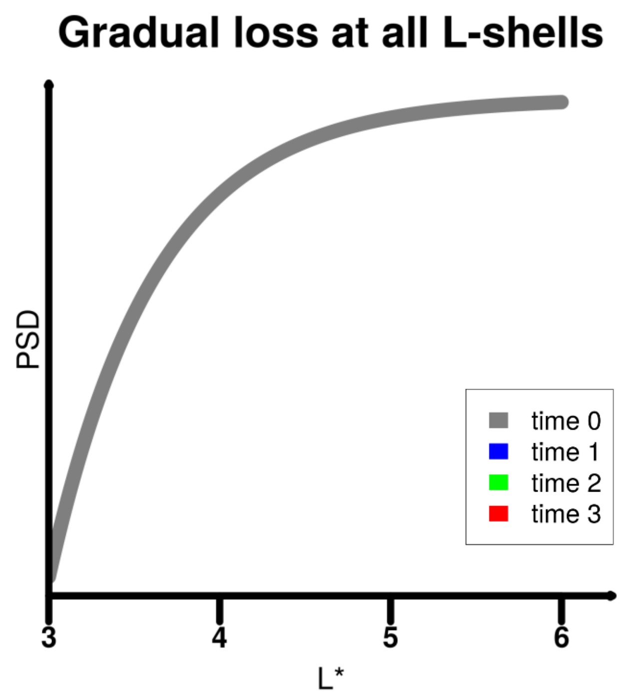

[Shprits et al., 2017, ***GRL***]

Three Scenarios of the Evolution of the PSD Profiles

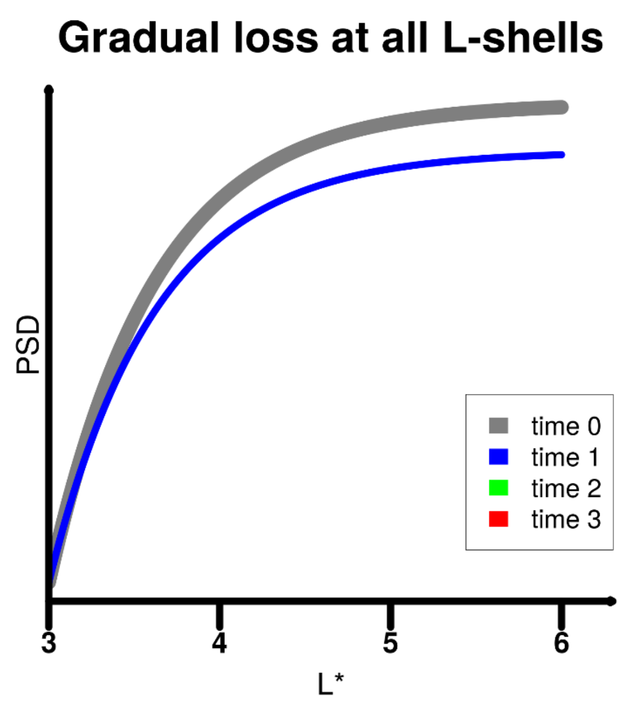

[Shprits et al., 2017, ***GRL***]

Three Scenarios of the Evolution of the PSD Profiles

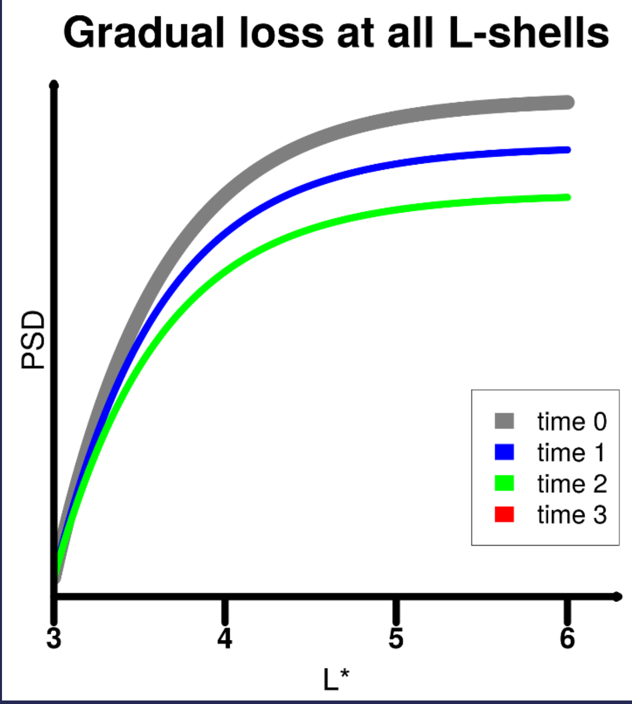

[Shprits et al., 2017, ***GRL***]

Three Scenarios of the Evolution of the PSD Profiles

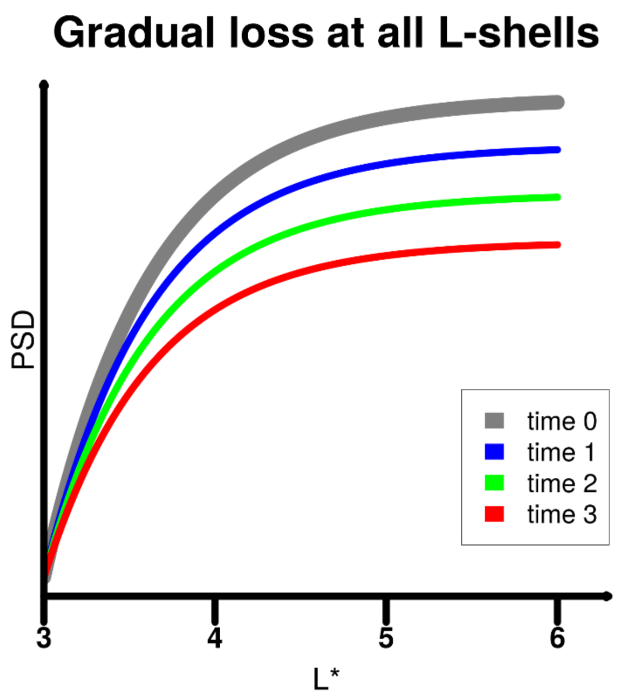

[Shprits et al., 2017, ***GRL***]

Three Scenarios of the Evolution of the PSD Profiles

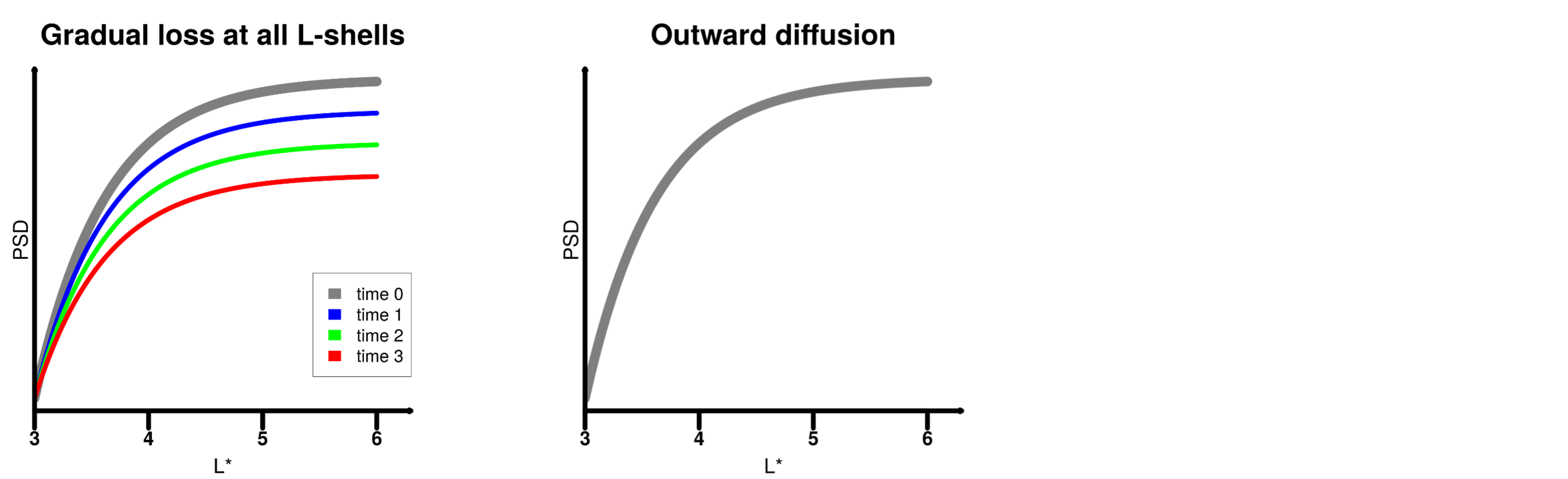

[Shprits et al., 2017, ***GRL***]

Three Scenarios of the Evolution of the PSD Profiles

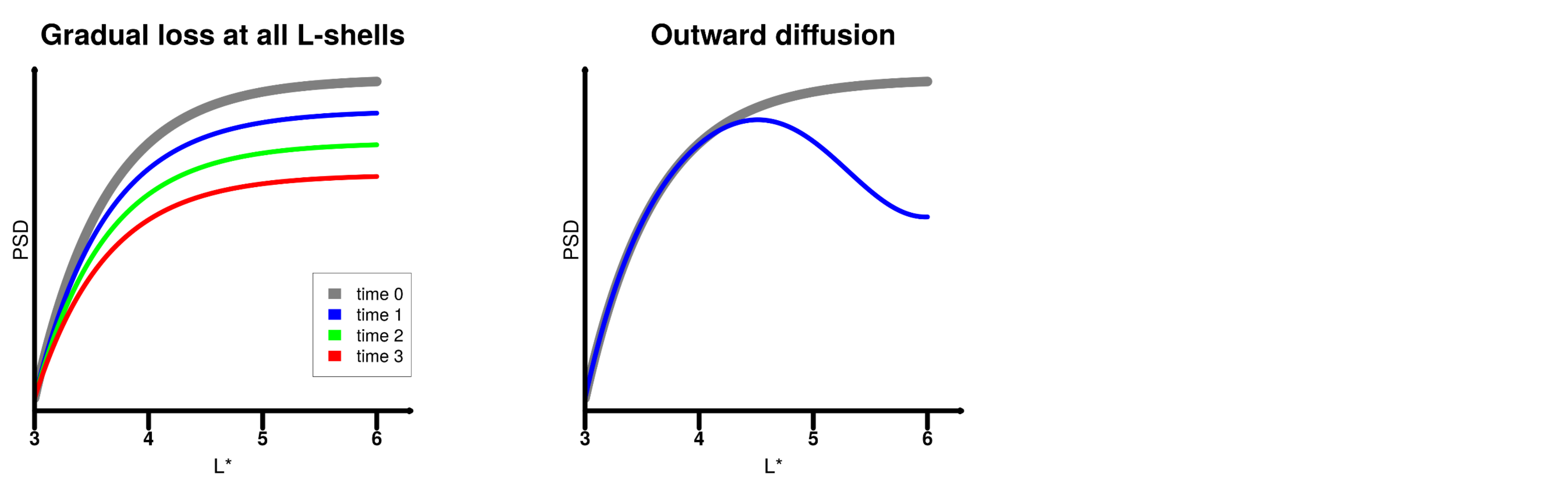

[Shprits et al., 2017, ***GRL***]

Three Scenarios of the Evolution of the PSD Profiles

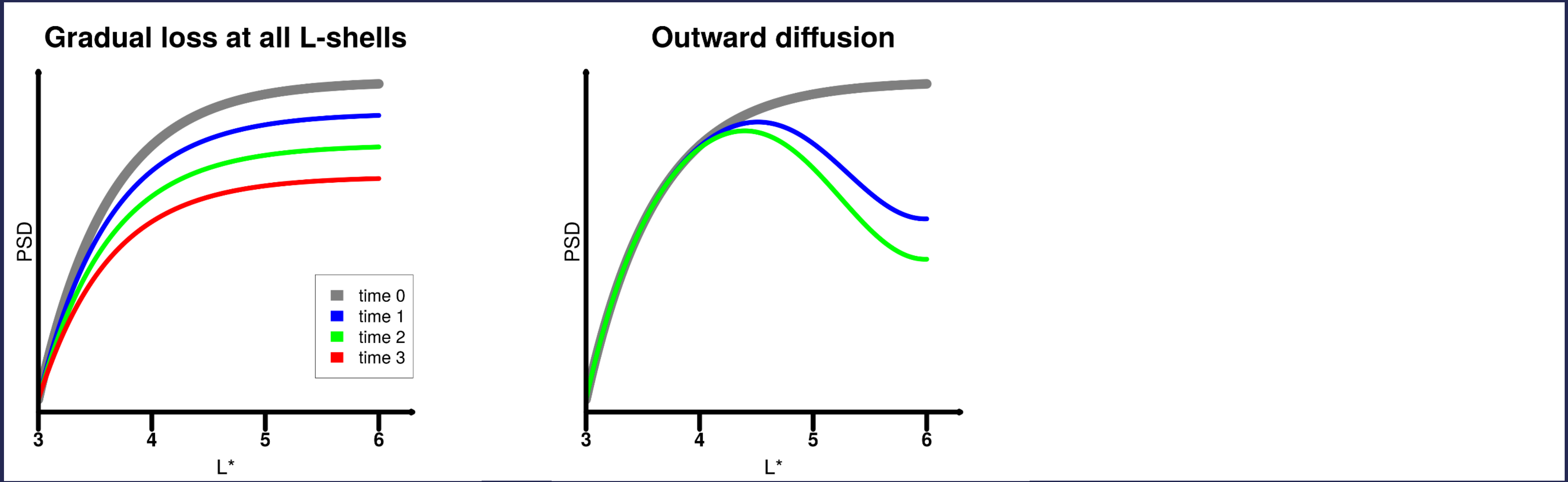

[Shprits et al., 2017, ***GRL***]

Three Scenarios of the Evolution of the PSD Profiles

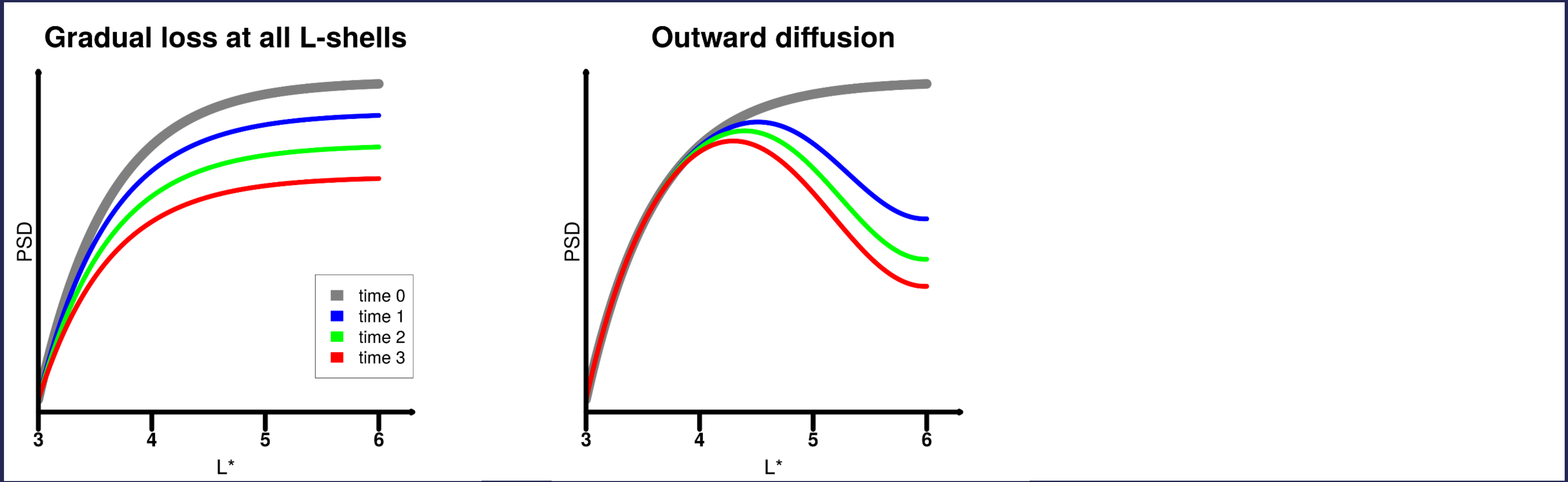

[Shprits et al., 2017, ***GRL***]

Three Scenarios of the Evolution of the PSD Profiles

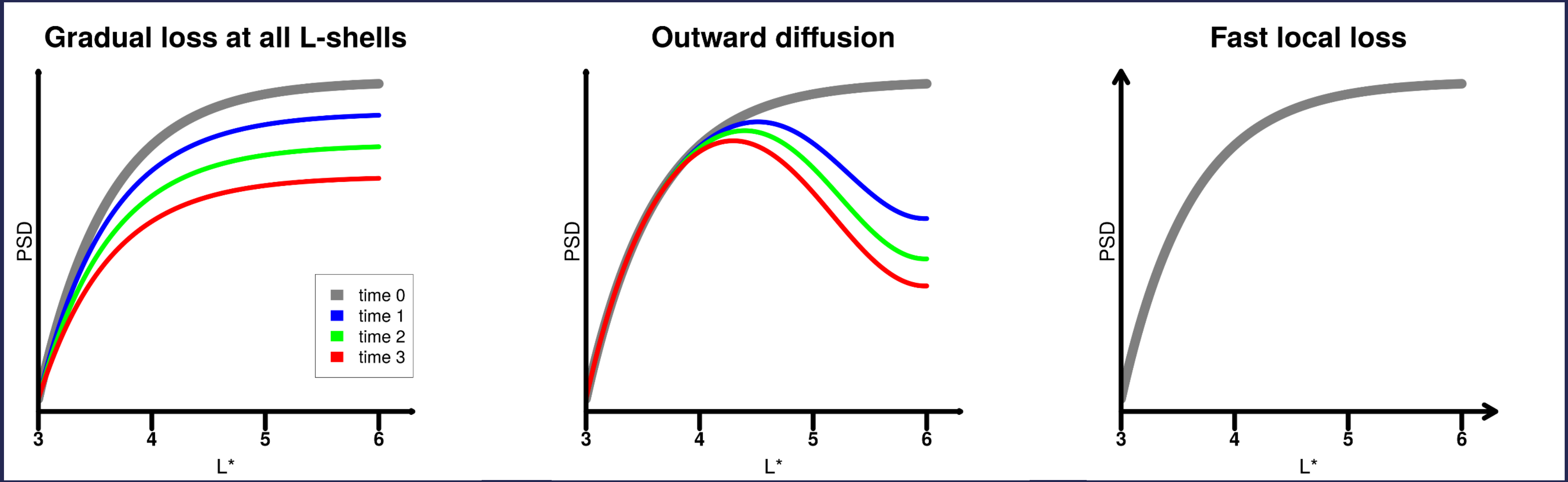

[Shprits et al., 2017, ***GRL***]

Three Scenarios of the Evolution of the PSD Profiles

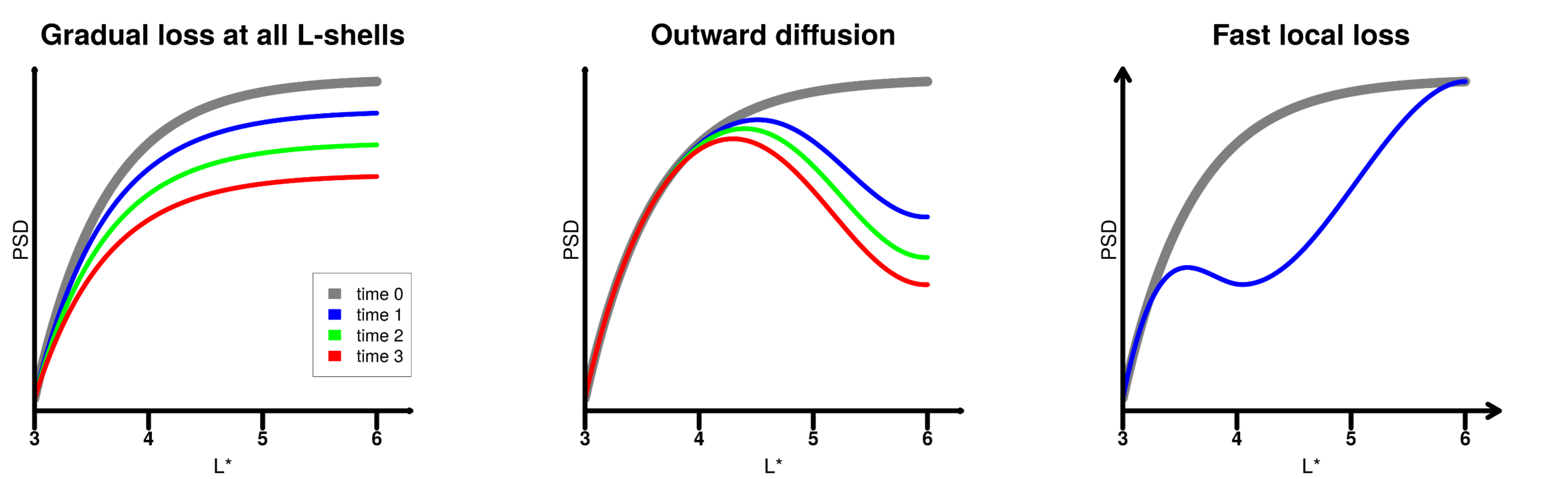

[Shprits et al., 2017, ***GRL***]

Three Scenarios of the Evolution of the PSD Profiles

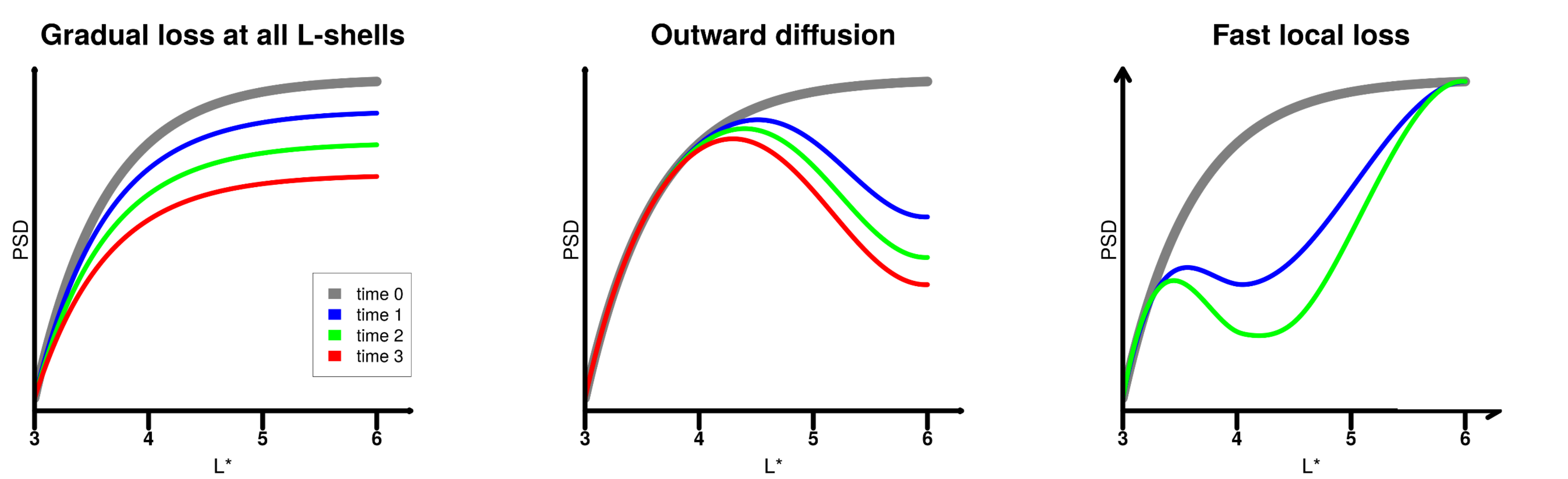

[Shprits et al., 2017, ***GRL***]

Three Scenarios of the Evolution of the PSD Profiles

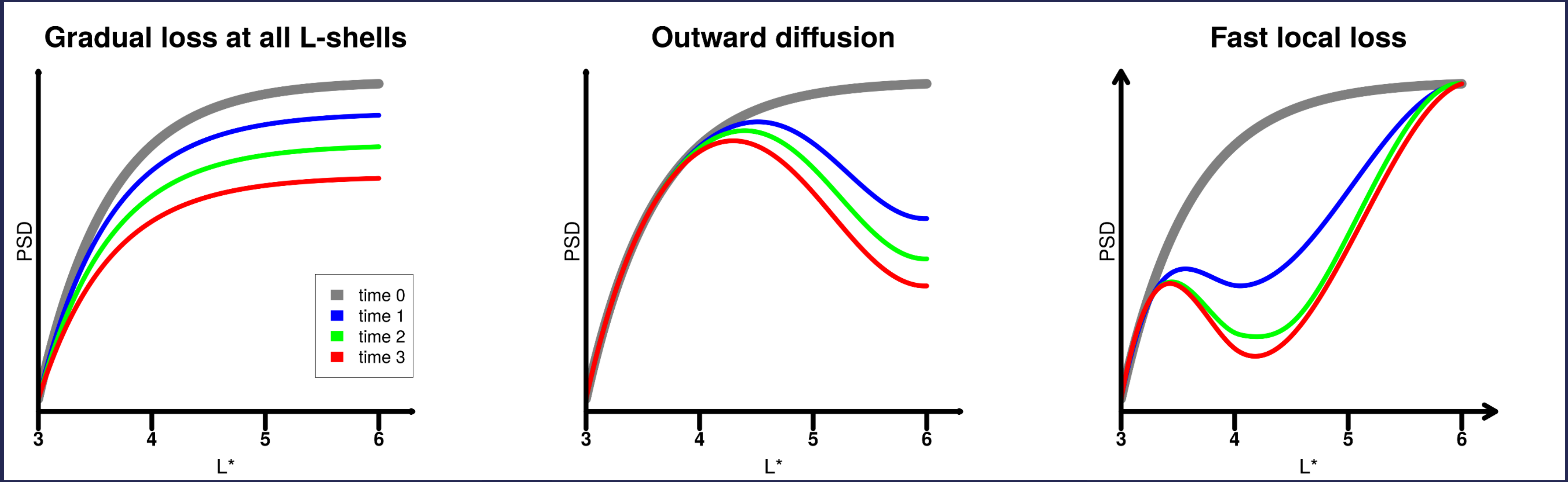

[Shprits et al., 2017, ***GRL***]

Deepening Minimums in PSD at Ultra-relativistic Energies

During the January 17, 2013 Profiles of PSD are monotonic at MeV energies.

Profiles of PSD show deepening local minimum for all considered magnetic fields models.

Such evolution of PSD is consistent with EMIC-induced scattering of ultra-relativistic electrons into the loss cone.

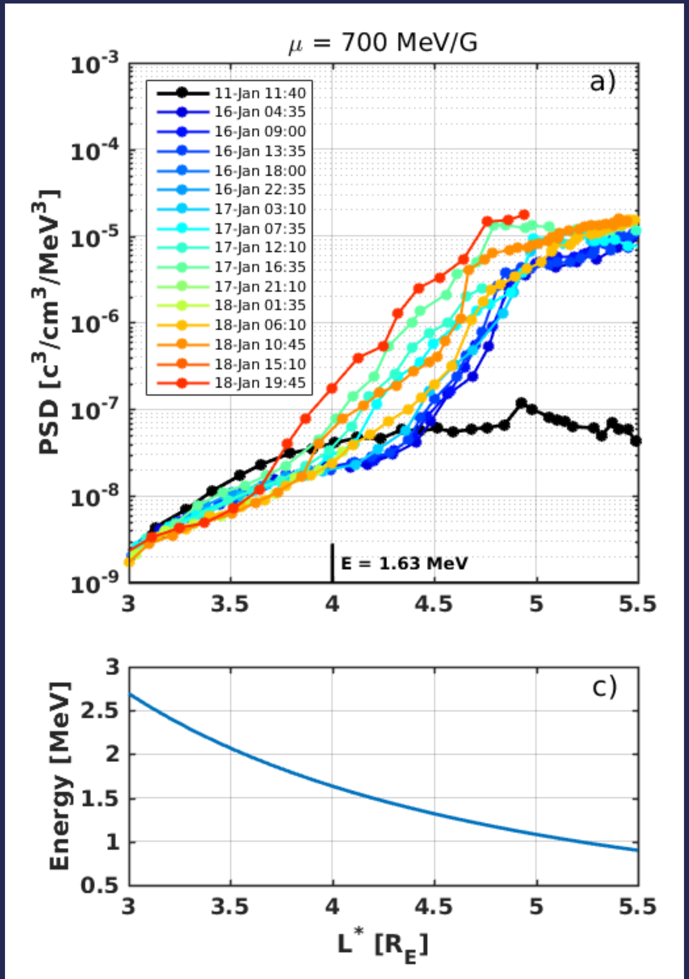

[Shprits et al., 2017, *GRL*]

Deepening Minimums in PSD at Ultra-relativistic Energies

During the January 17, 2013 Profiles of PSD are monotonic at MeV energies.

Profiles of PSD show deepening local minimum for all considered magnetic fields models.

Such evolution of PSD is consistent with EMIC-induced scattering of ultra-relativistic electrons into the loss cone.

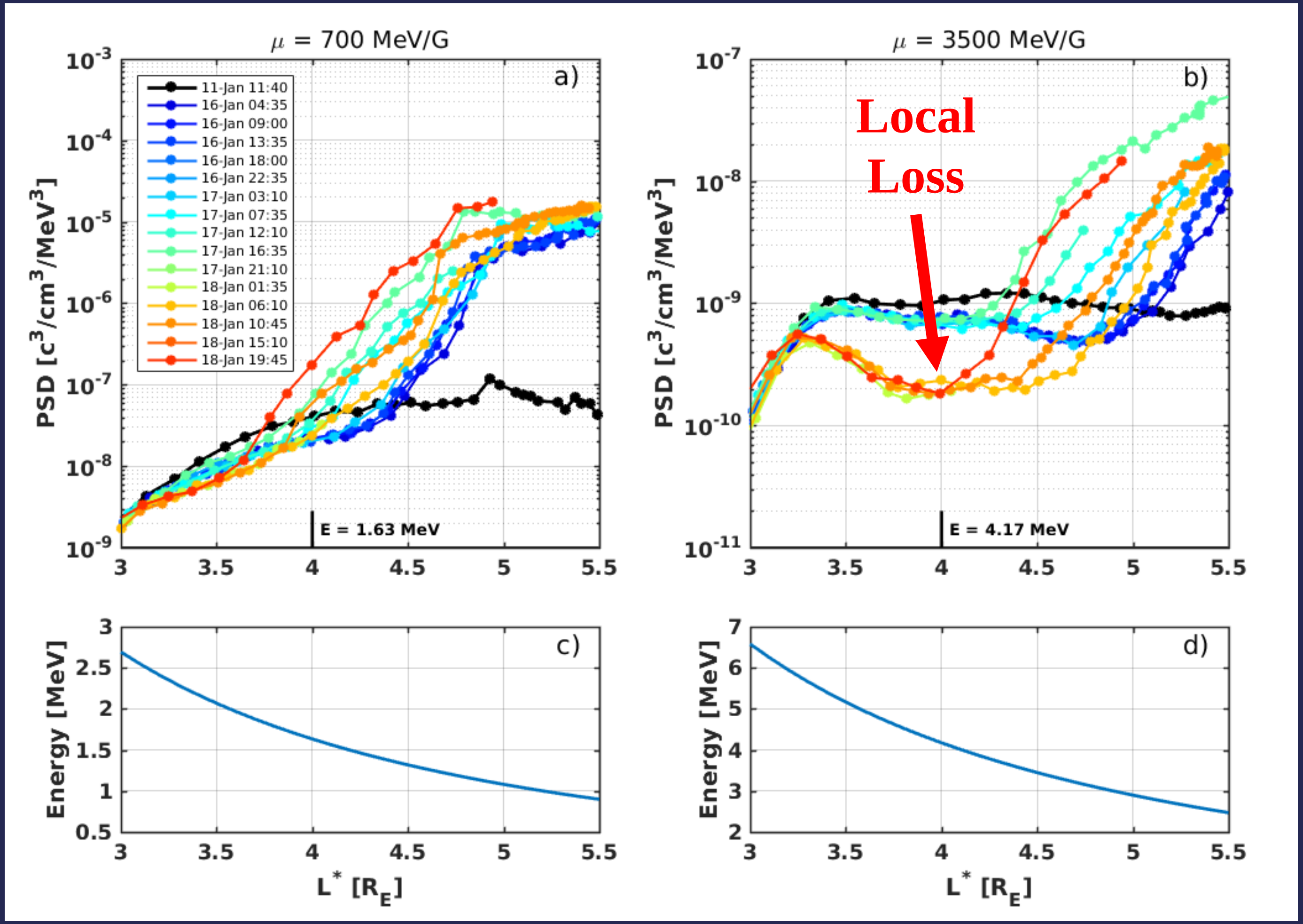

[Shprits et al., 2017, *GRL*]

Profiles of PSD for Different Values of the First Invariant

At lower energies, profiles are monotonic.

Deeps in PSD are observed at E>~2MeV and deepen with increasing energy.

μ = 300MeV/G μ = 500MeV/G μ = 700MeV/G μ = 1500MeV/G μ = 2500MeV/G μ = 3500MeV/G

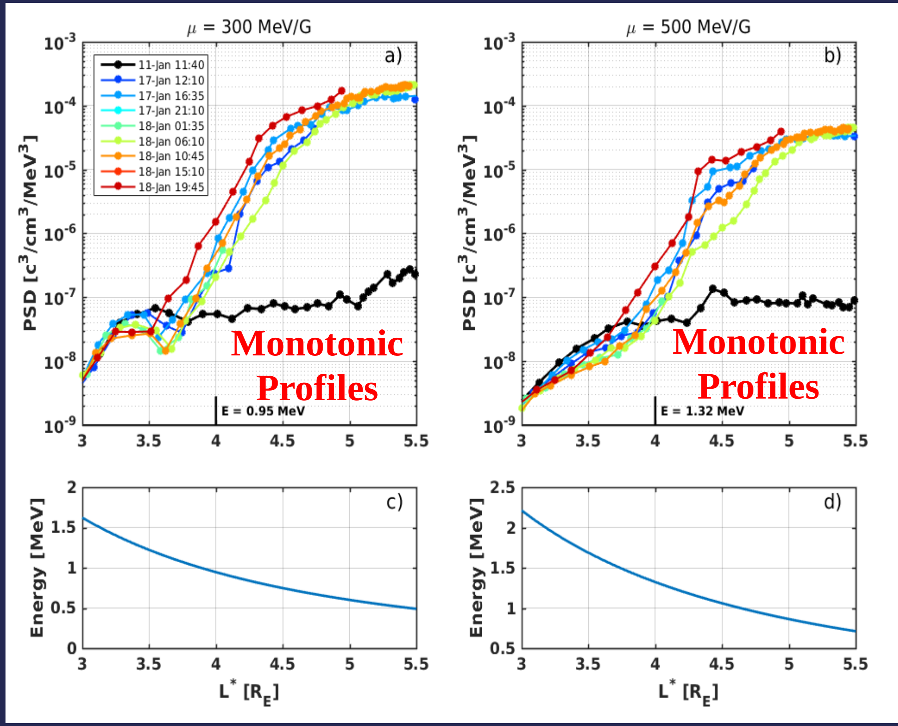

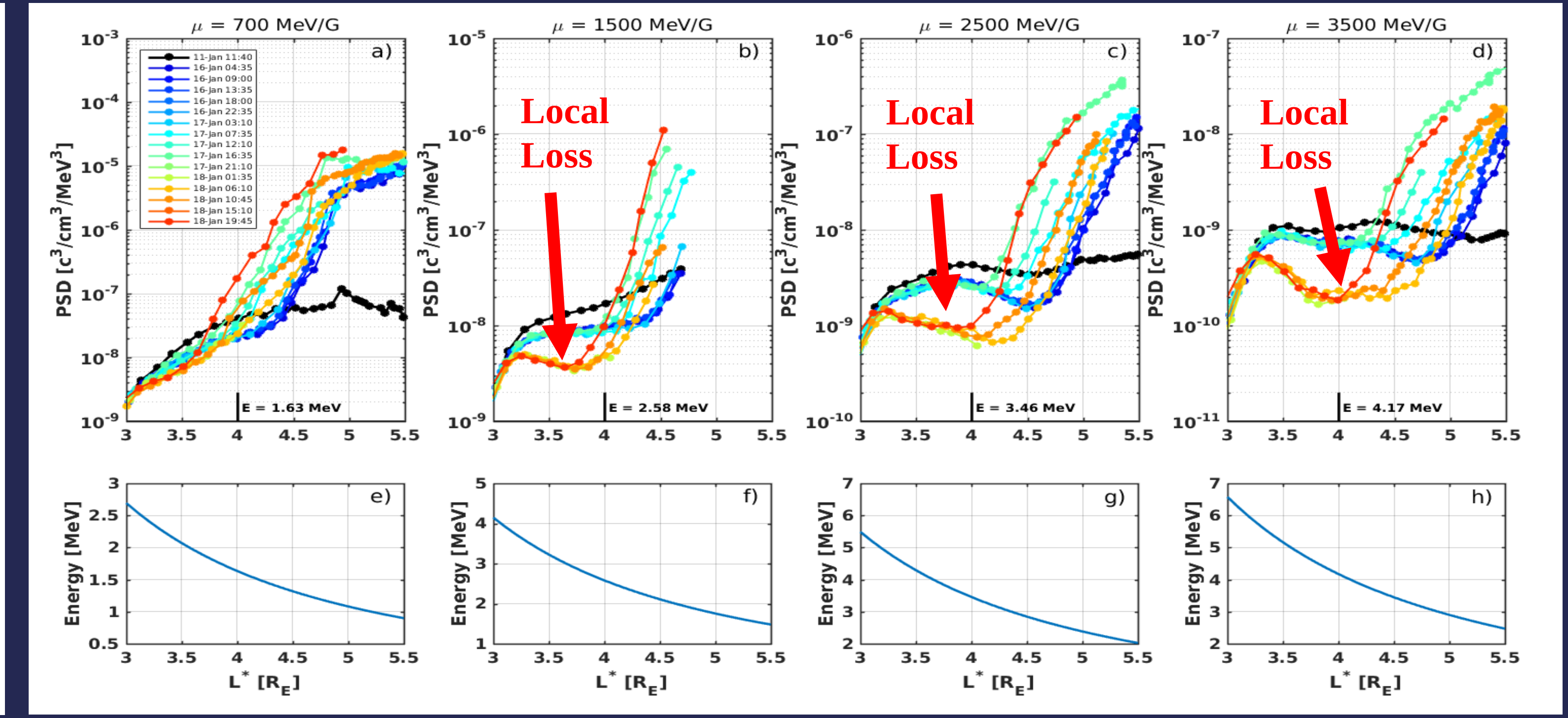

[Shprits et al., 2017, *GRL*]

Dynamic Evolution of Deeps in PSD

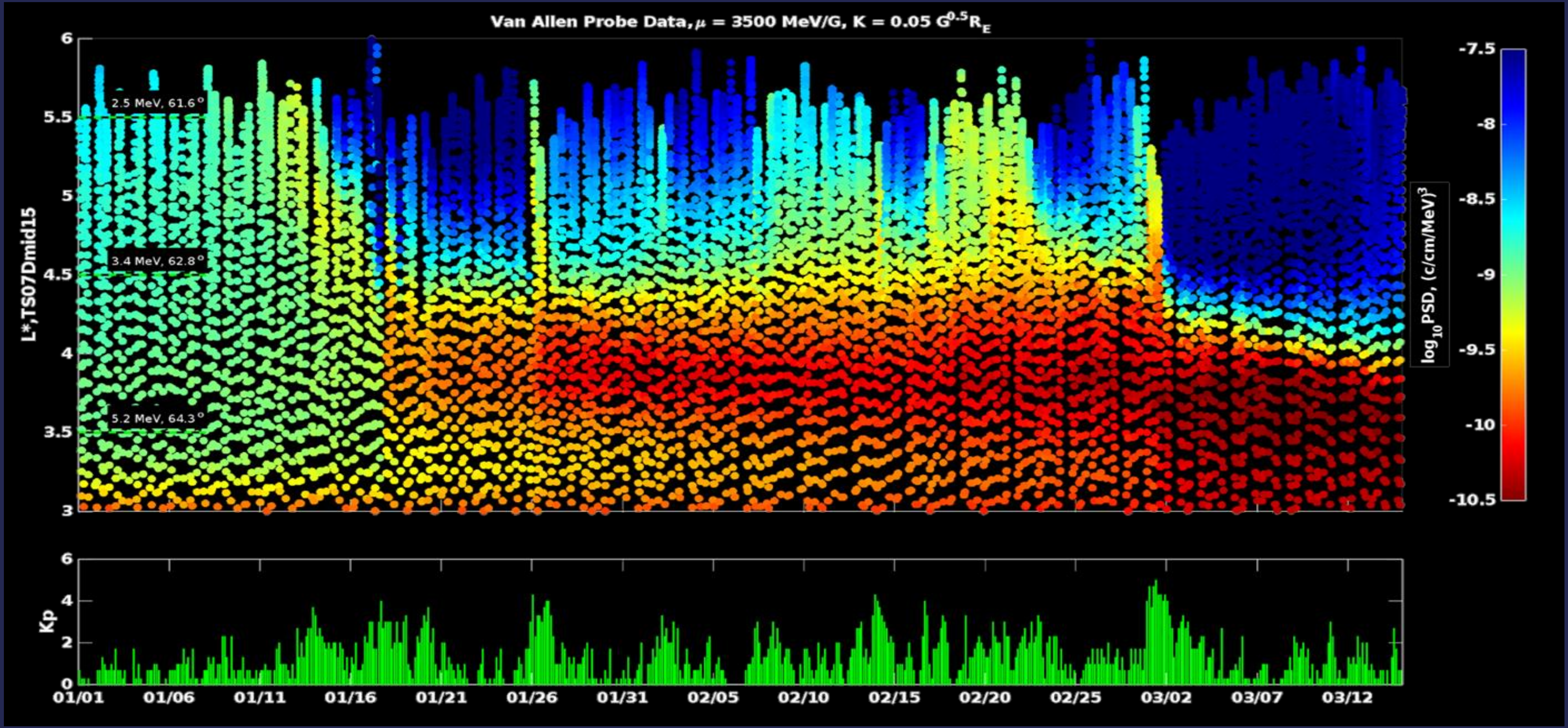

[Shprits et al., 2017, *GRL*]

Evidence for EMIC Scattering

Deeps in PSD correlate with Wave Observations and narrowing of pitch angle distributions

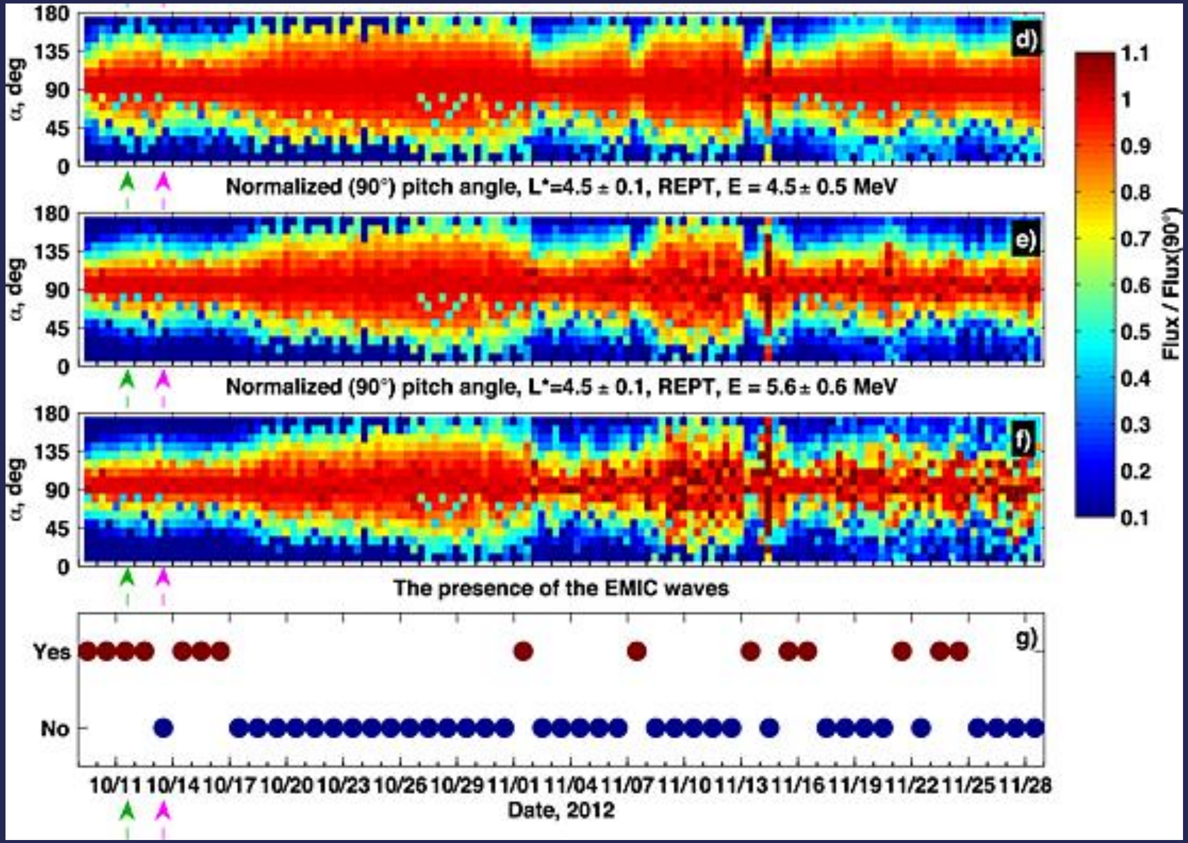

[Usanova et al., 2014, *GRL*]

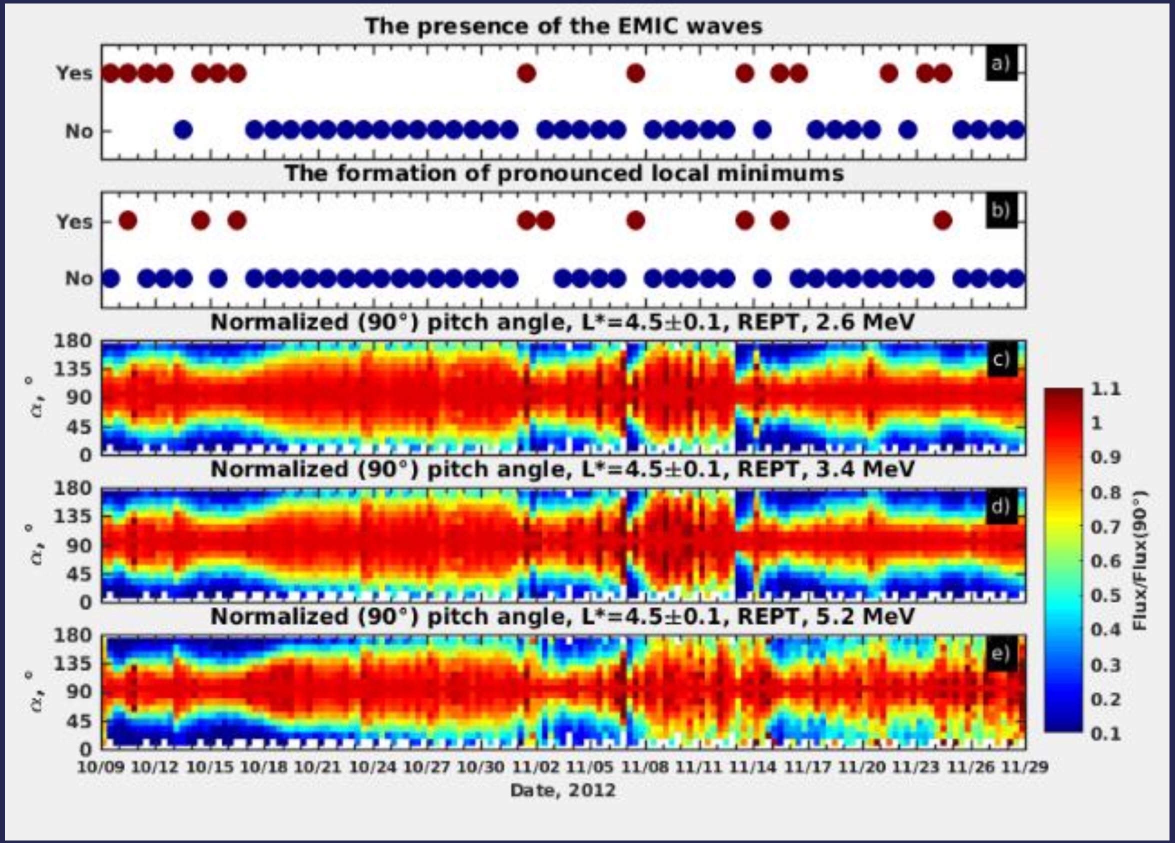

[Aseev et al., 2017, *JGR*]

Simulations of the "Storage Ring" without EMIC waves

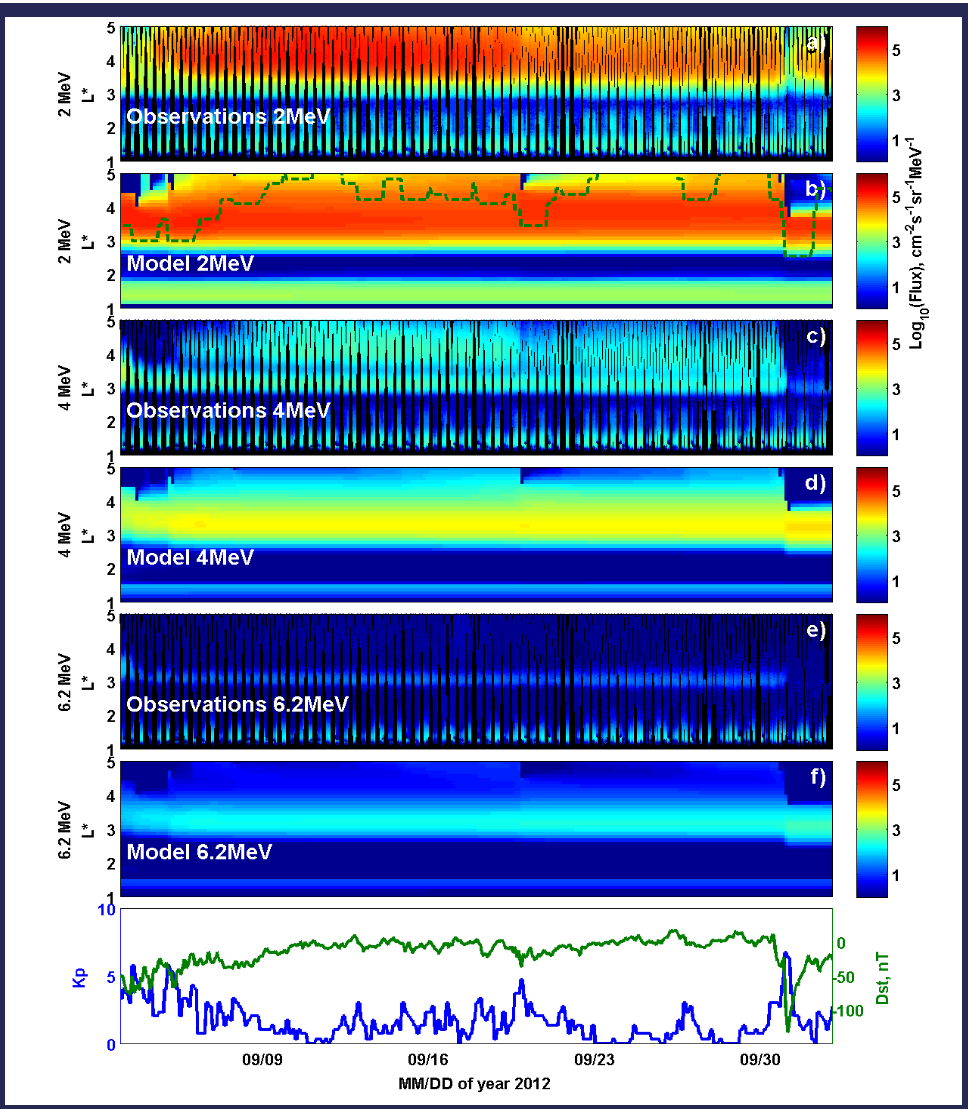

Simulations without EMIC wave scattering can reproduce 2MeV dynamics but fail to reproduce the 3 zone structure and the narrow ring formed at higher energies.

Radial diffusion can only smoth gradients and can not produce sharp dropouts and very narrow strucutres.

[Shprits et al., 2013, *Nature Physics*]

Simulations of the “Storage Ring”

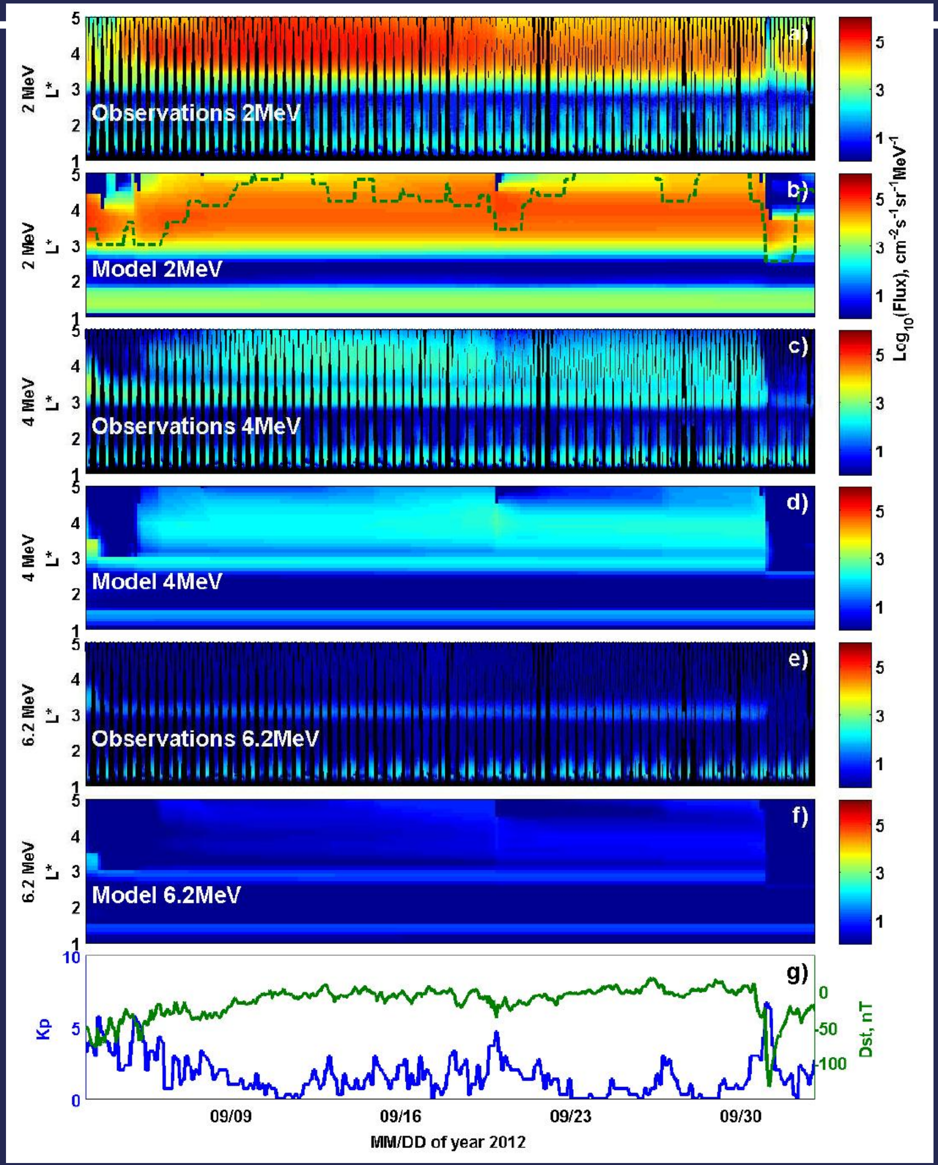

- Simulations with EMIC wave scattering can reproduce unusual behavior of the radiation belts.

  Simulations with EMIC scattering reproduces 3 zone structure at 4MeV and a very narrow remnant belt at 6.2 MeV.

  Simulations without EMIC waves can not reproduce such narrow remnant belts.

[Shprits et al., 2013, *Nature Physics*]

PSD Profiles During September 2012 Storm

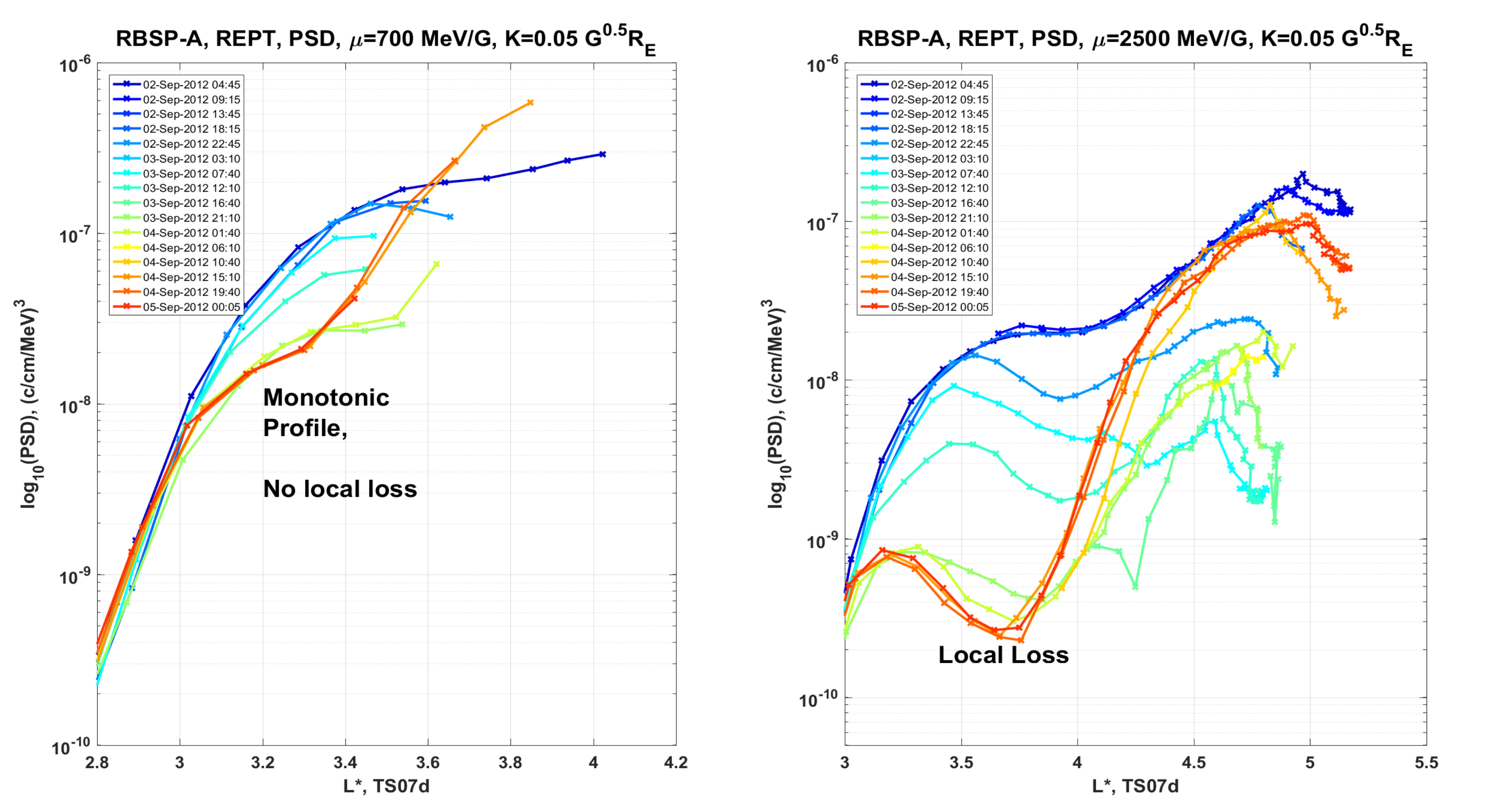

Deeps in PSD confirm conclusions of modeling by Shprits et al. [2015]

[Shprits et al., 2018, *Nature Physics*]

Theoretic Estimates of the Minimum Resonance Energies

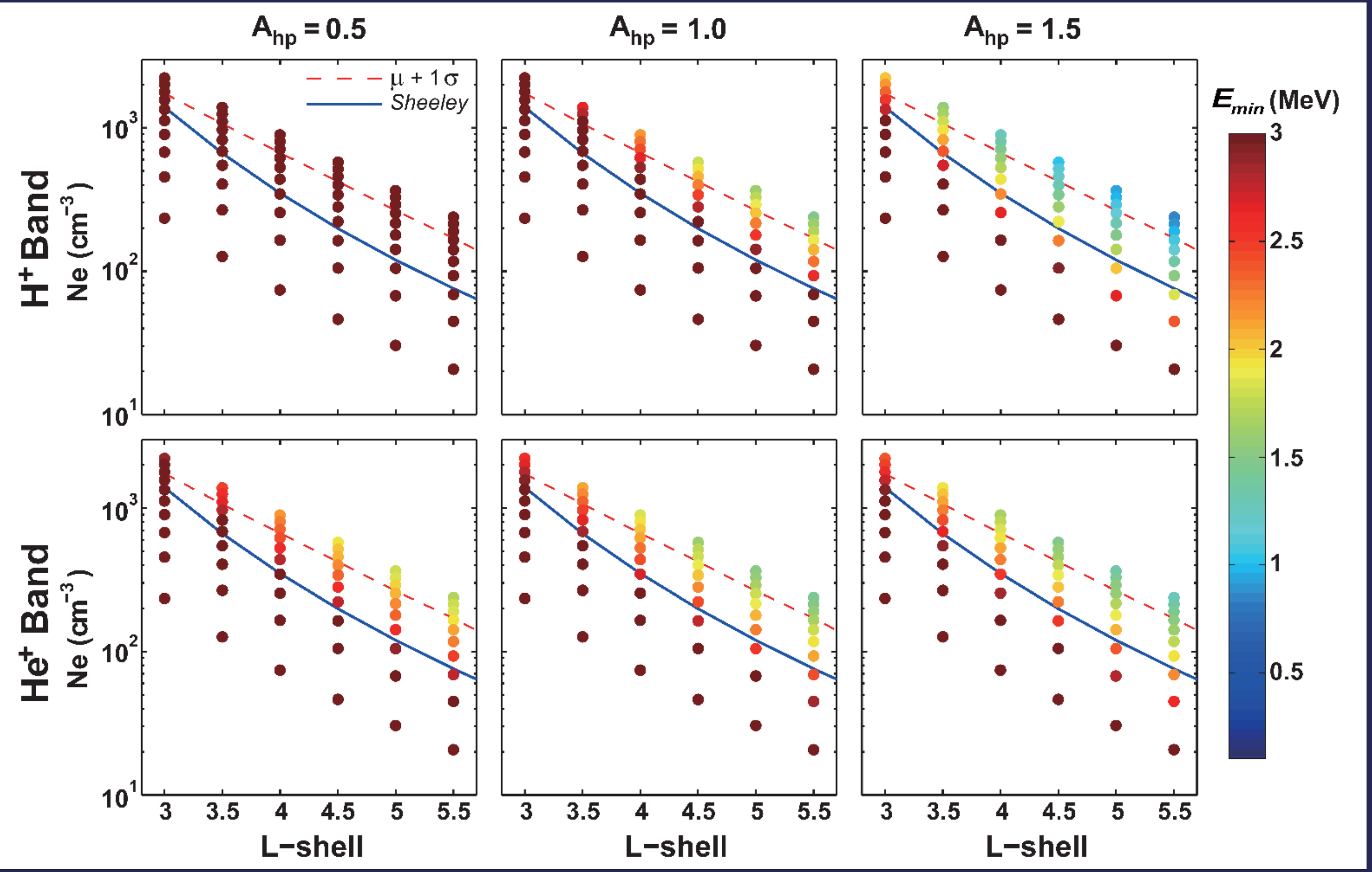

[Cao*, Shprits*, Ni and Zhelavskaya, 2017, *Scientific Reports*]

For realistic values of anisotropy, density and various combinations of ion composition calculations including hot plasma effects result in resonance energies above ~2 MeV .

Theoretic Estimates of the Minimum Resonance Energies

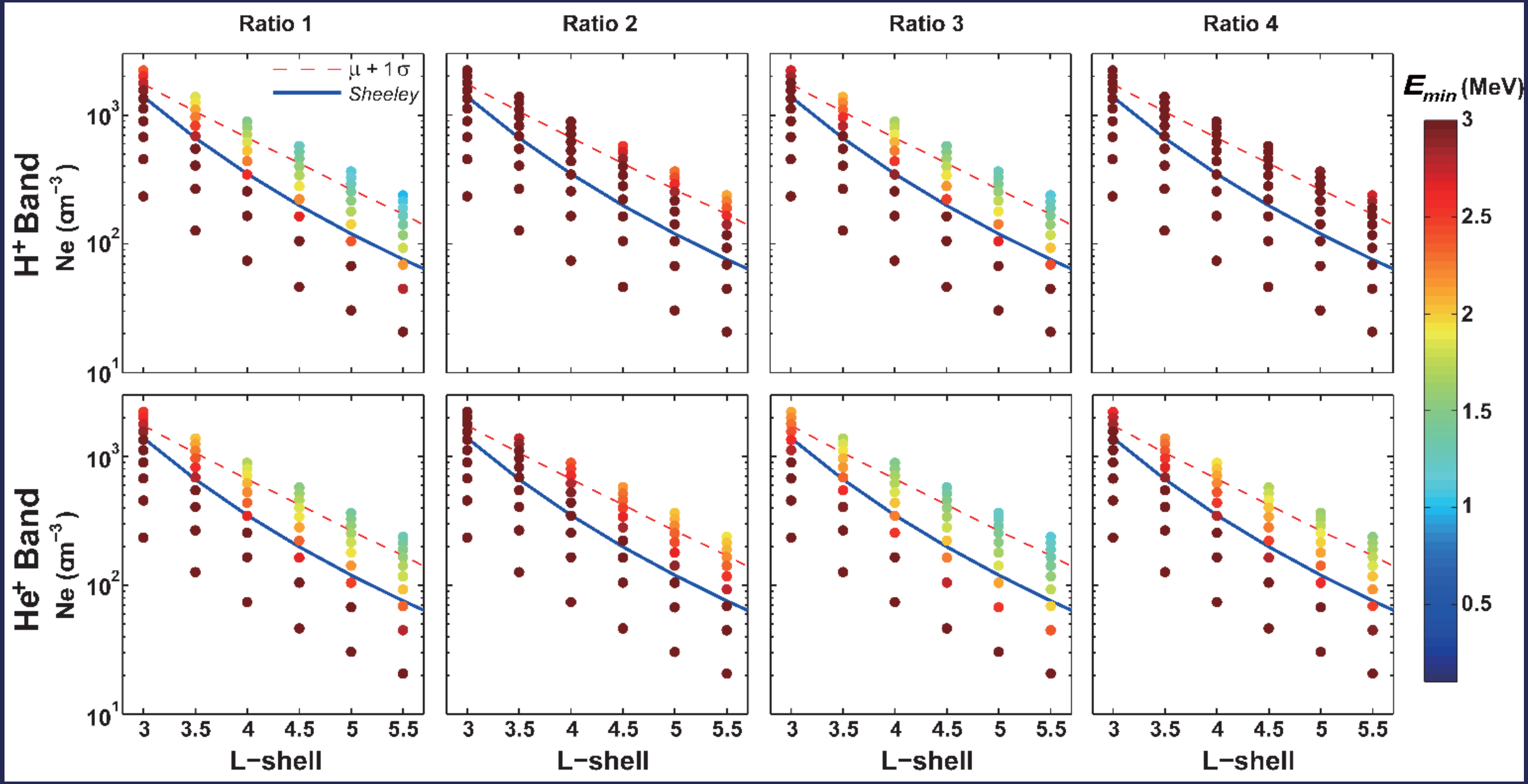

[Cao*, Shprits*, Ni and Zhelavskaya, 2017, *Scientific Reports*]

Summary

- While EMIC waves do not substantially change the dynamics of the relativistic electrons, at ultra-relativistic energies, scattering by EMIC waves start to play a crucial role.
- Knife-edge dropout at ultra-relativistic energies, pitch angle distributions with bite-outs at small pitch angles and clear differences between relativistic and ultra-relativistic dynamics all show that EMIC waves play a dominant role in scattering ultra-relativistic electrons.
- Scattering by EMIC waves explains the formation of a narrow belt that lasted for approximately 1 month in September 2012.
- Deepening minimums in PSD provide additional evidence for the loss at ultra-relativistic energies and regions where EMIC-induced loss depletes ultra-relativistic electrons.
- Estimates of MRE that account for realistic plasma density, composition, anisotropy, and density show that resonances below 2 MeV are unlikely.
- Ultra-relativistic electrons form a new population of the belts that is driven by different physical processes [Shprits et al., 2013, *Nature Physics*].

Difference in Behavior of Ultra-relativistic and Relativistic Electron Fluxes

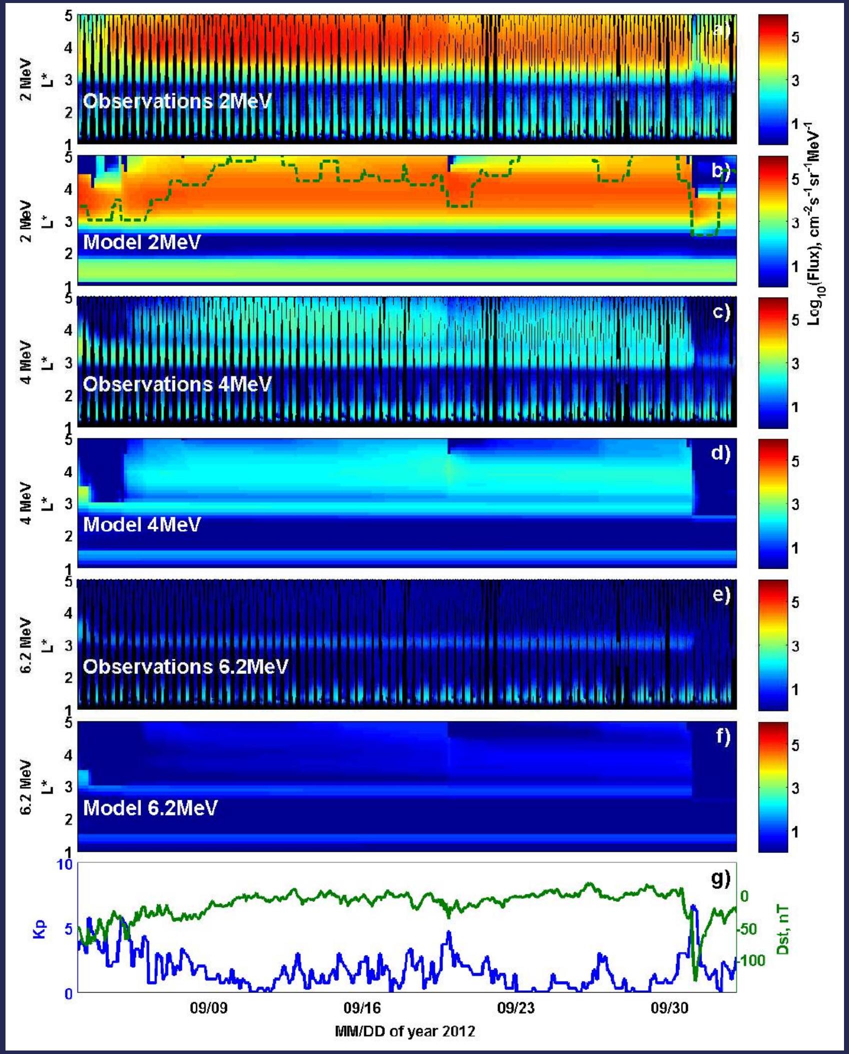

[Shprits et al., 2013, *Nature Physics*]

- Simulations with EMIC wave scattering can reproduce unusual behavior of the radiation belts.
- Simulations with EMIC scattering reproduces 3 zone structure at 4MeV and a very narrow remnant belt at 6.2 MeV.
- Simulations without EMIC waves can not reproduce such narrow remnant belts.

Analysis of PSD Profiles Presented by Mann et al. (2016)

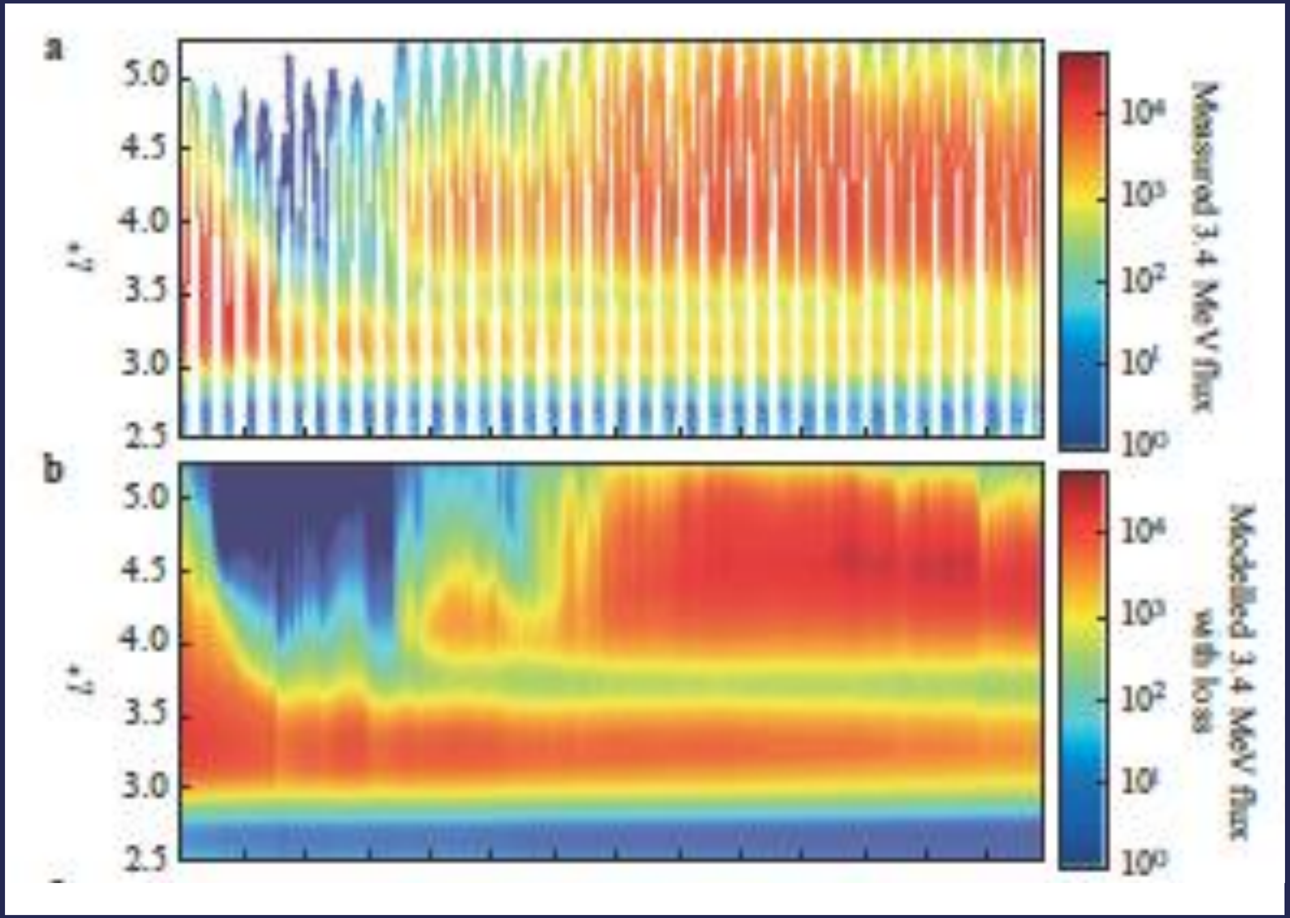

[Mann et al., 2016, *Nature Physics*]

- Simulations of Mann et al., 2012 show an order of magnitude higher fluxes than observed.
- The remnant belt is at least twice as wide as that of observed.
- The boundary condition of zero PSD at 5.5. is unrealistic.
- Simulations are only presented for a narrow range of energies.

Simulations of Mann et al. (2018)

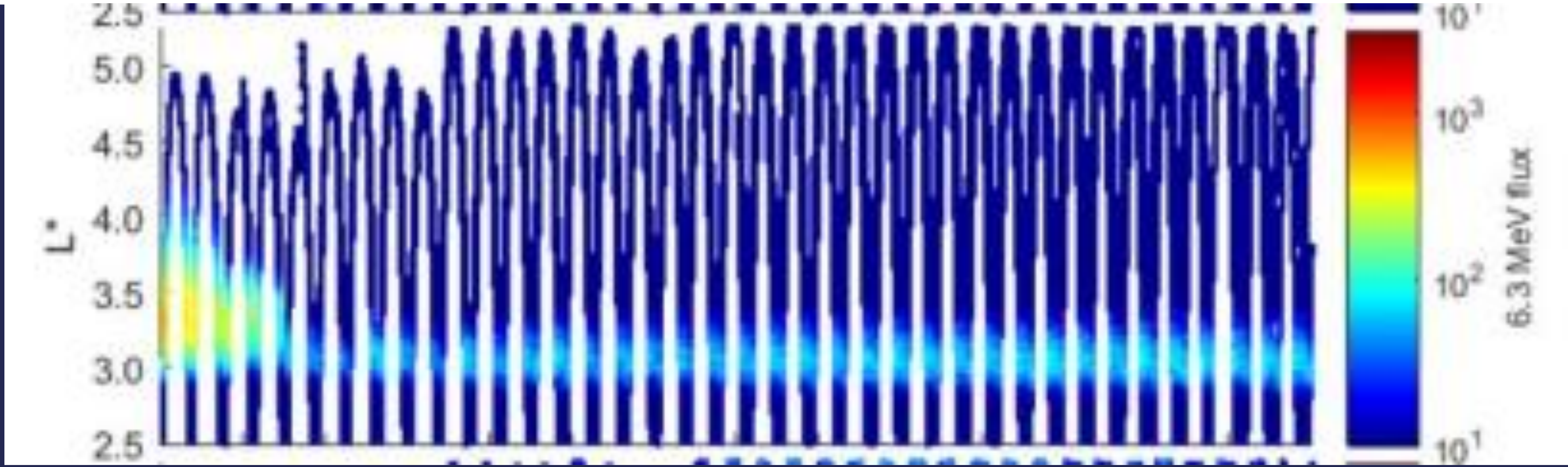

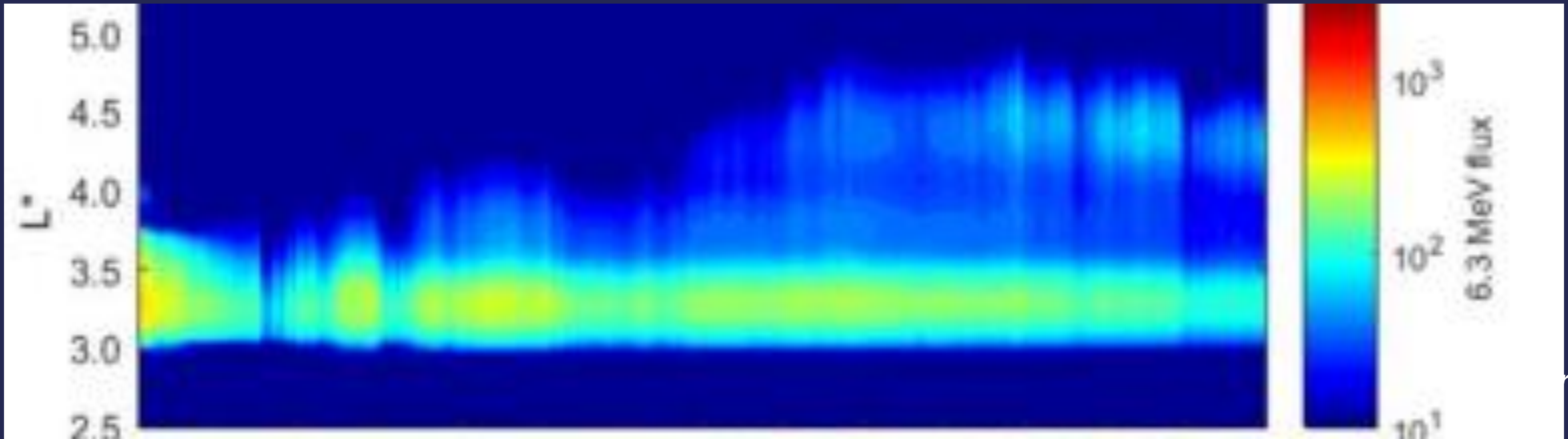

re Physics]

Mann et al. (2018)

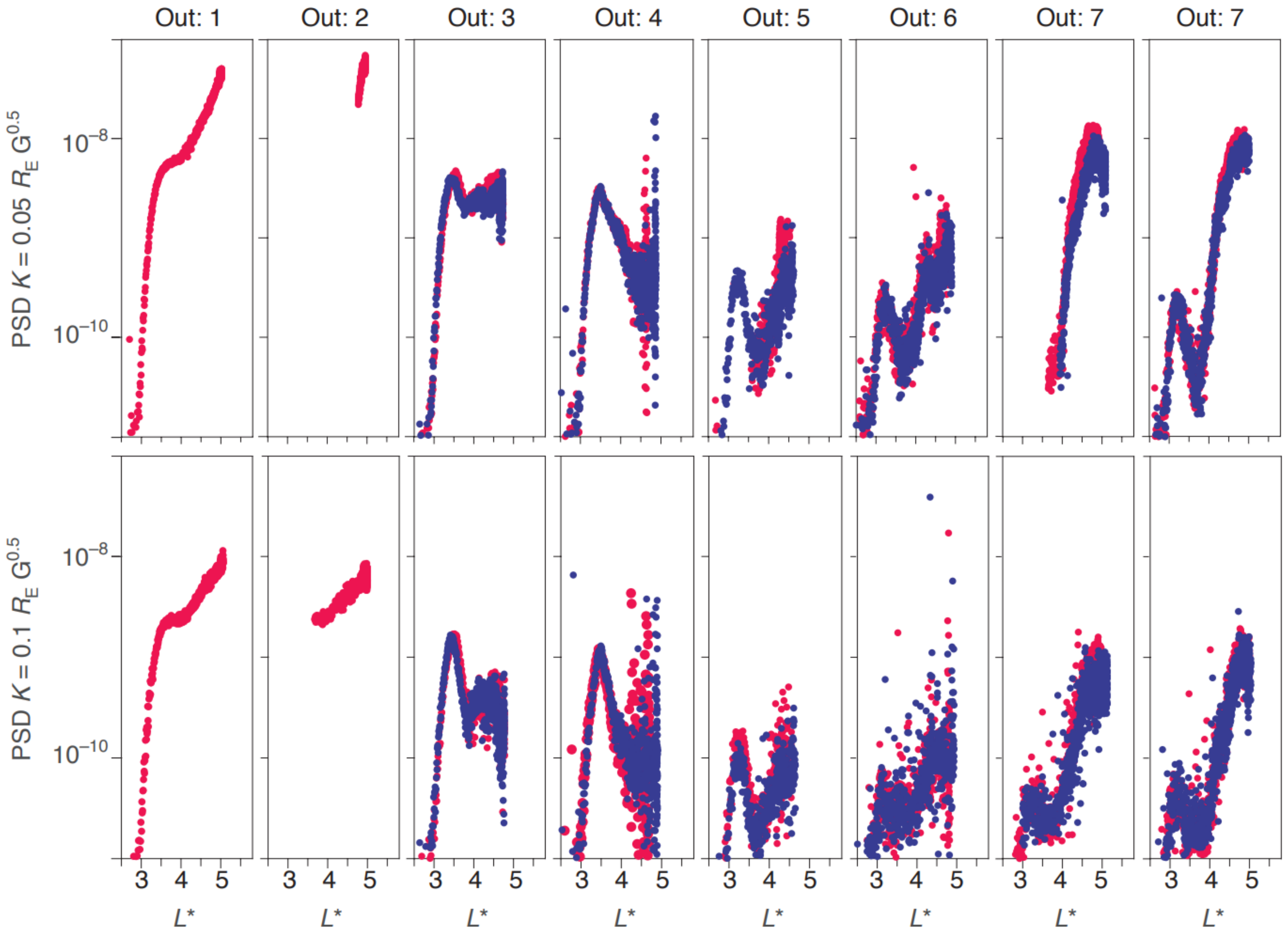

Mann et al. (2018)
K = 0.05

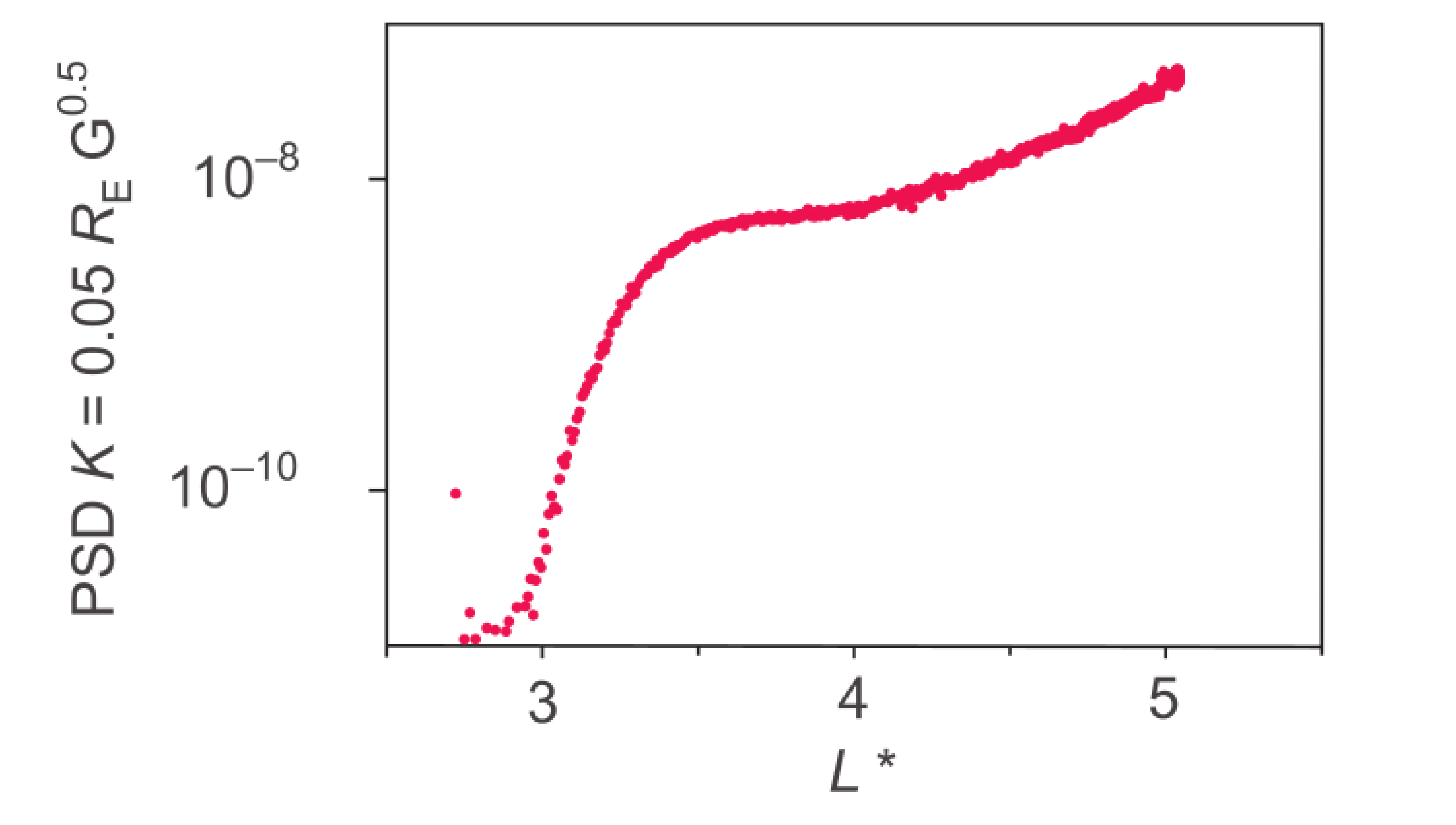

Mann et al. (2018)
K = 0.05

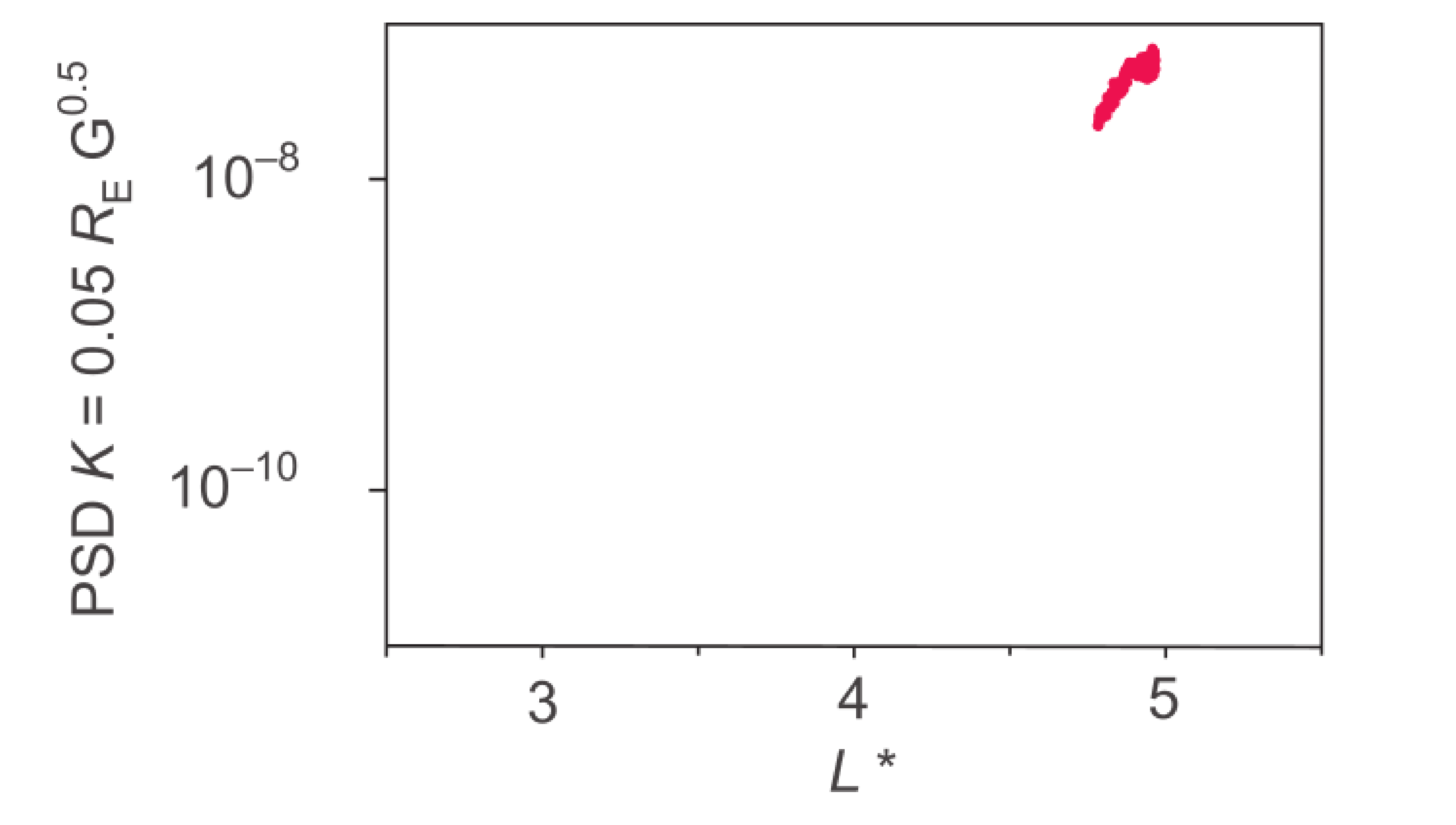

Mann et al. (2018)
K = 0.05

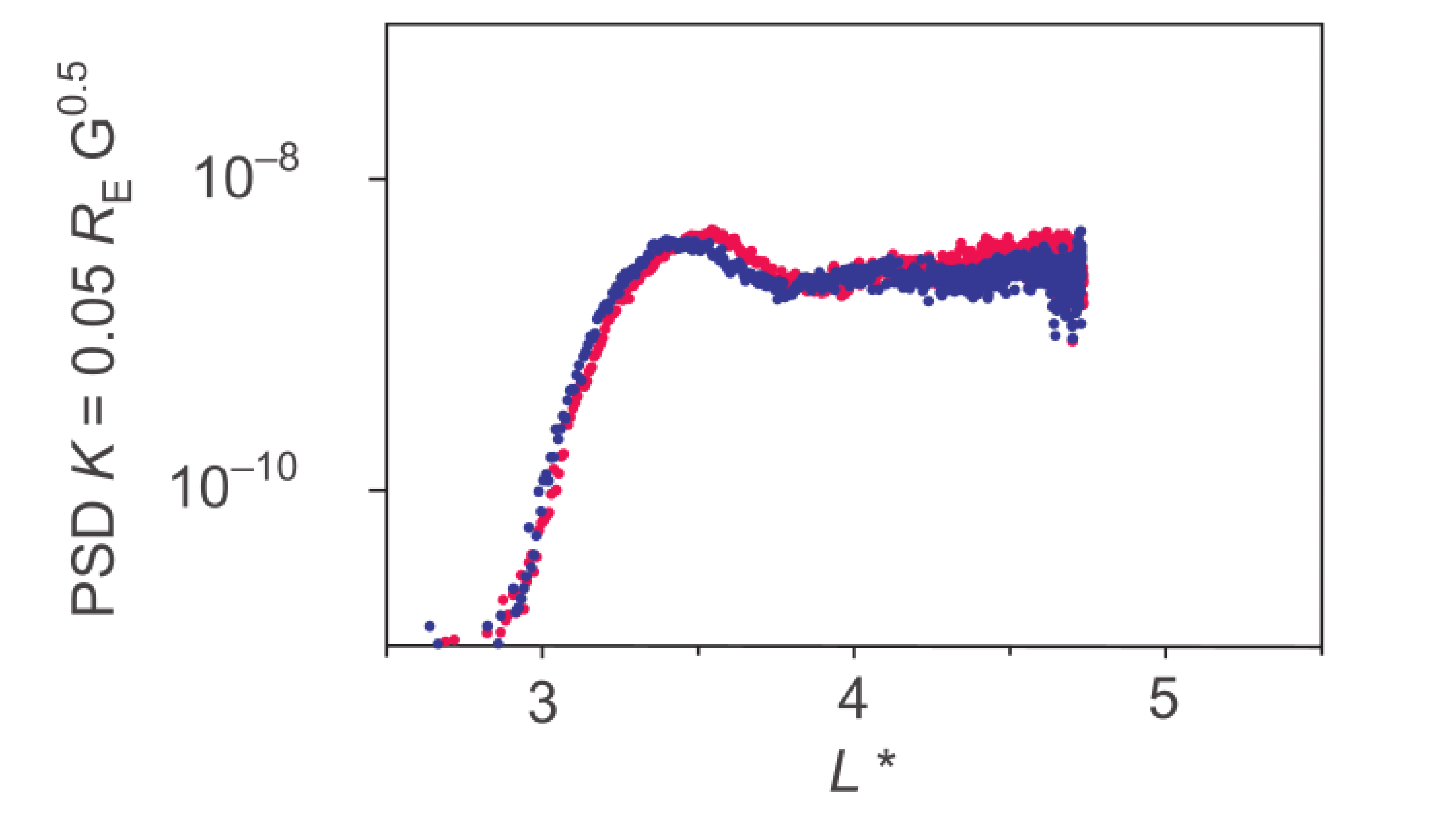

Mann et al. (2018)
K = 0.05

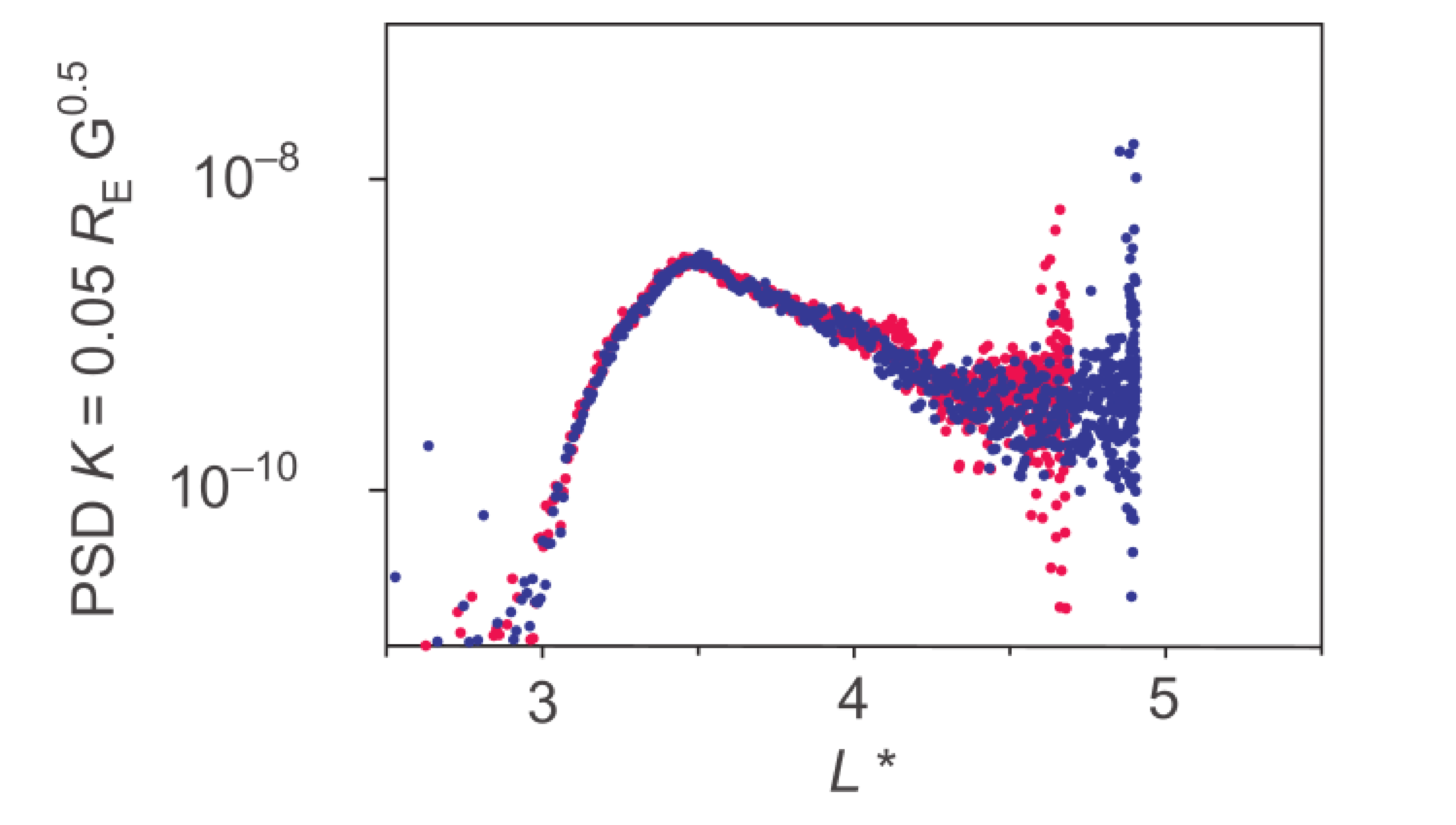

Mann et al. (2018)
K = 0.05

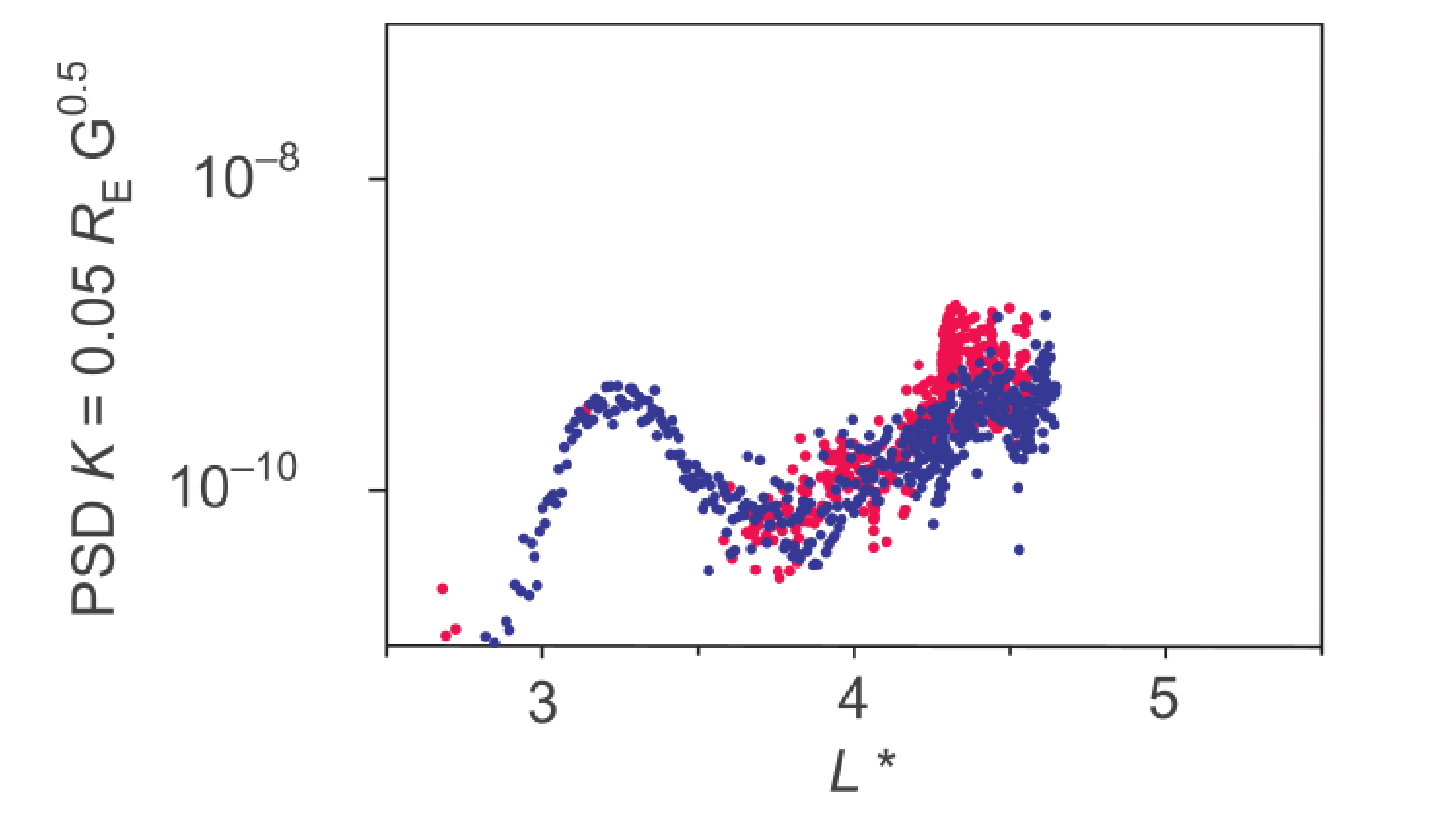

Mann et al. (2018)
K = 0.05

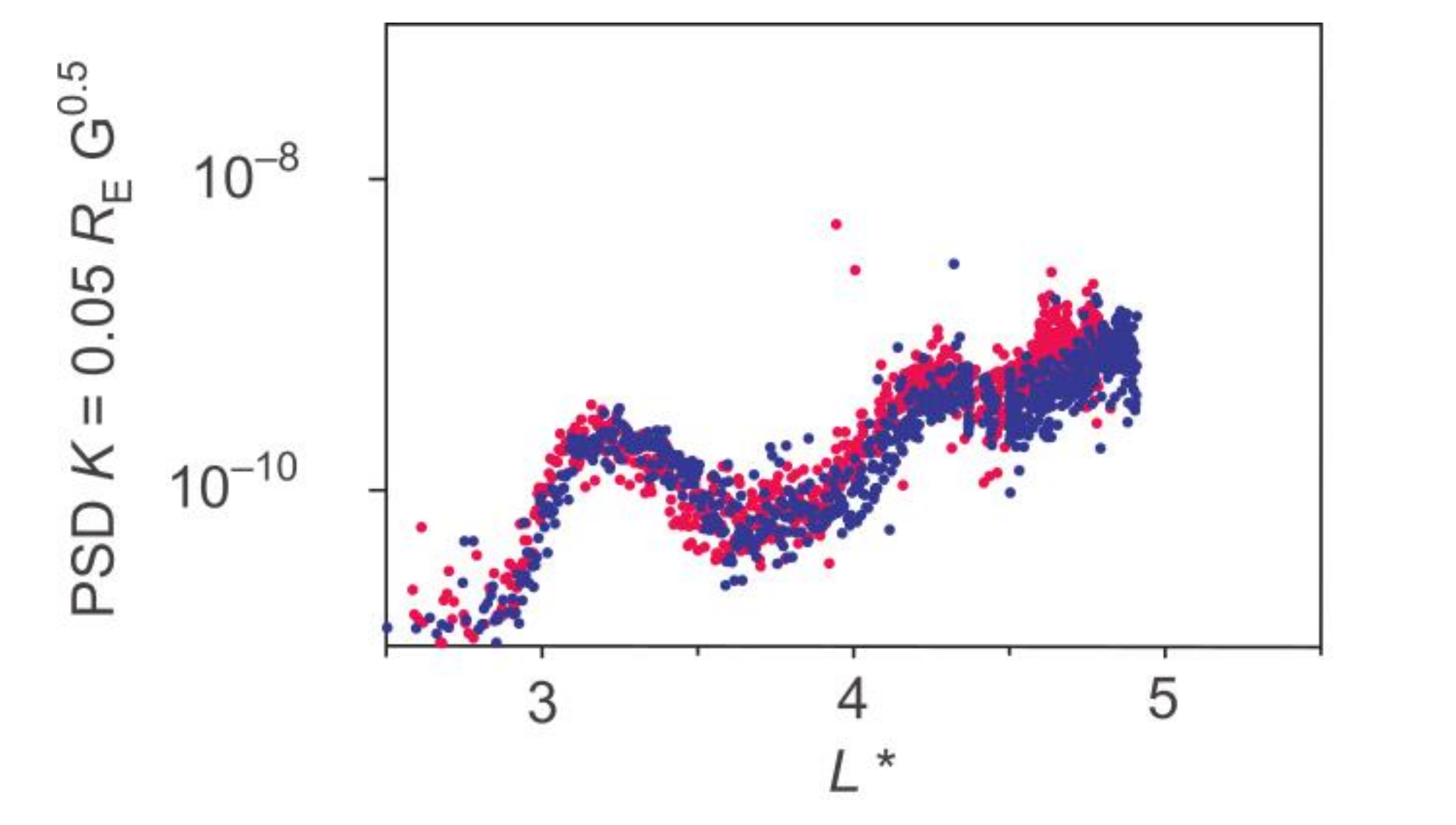

Mann et al. (2018)
K = 0.05

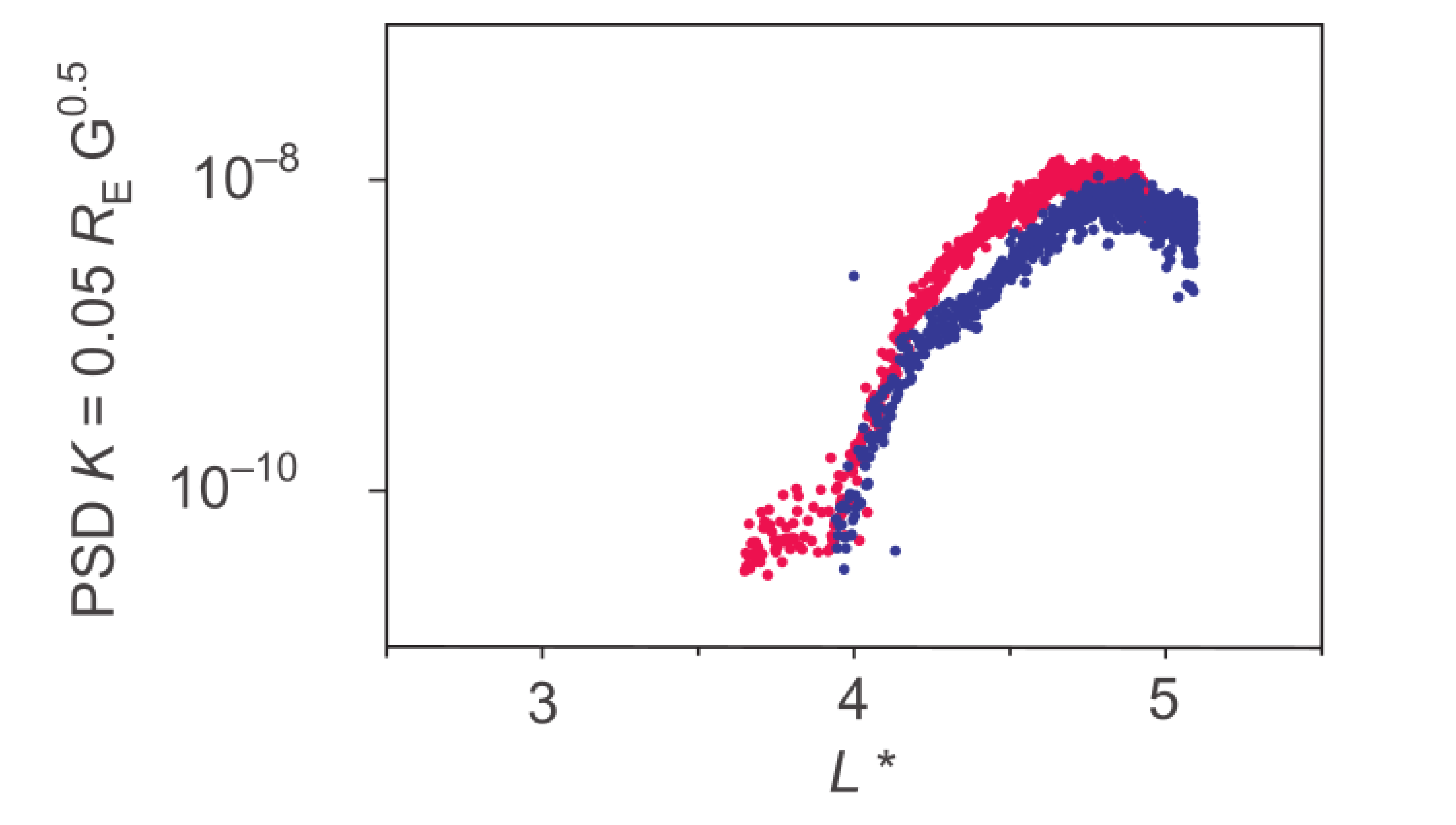

Mann et al. (2018)
K = 0.05

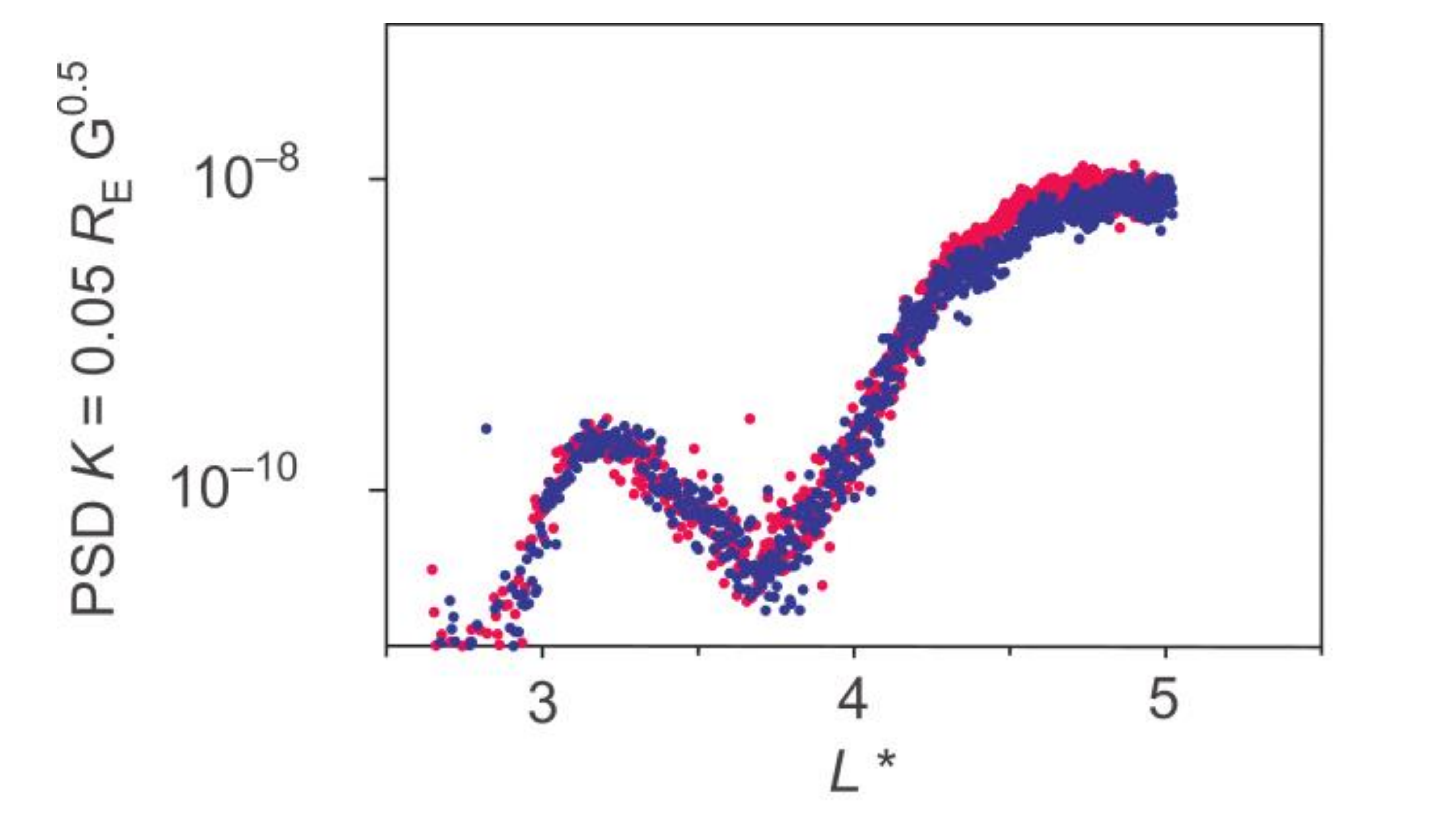

Mann et al. (2018)
K = 0.1

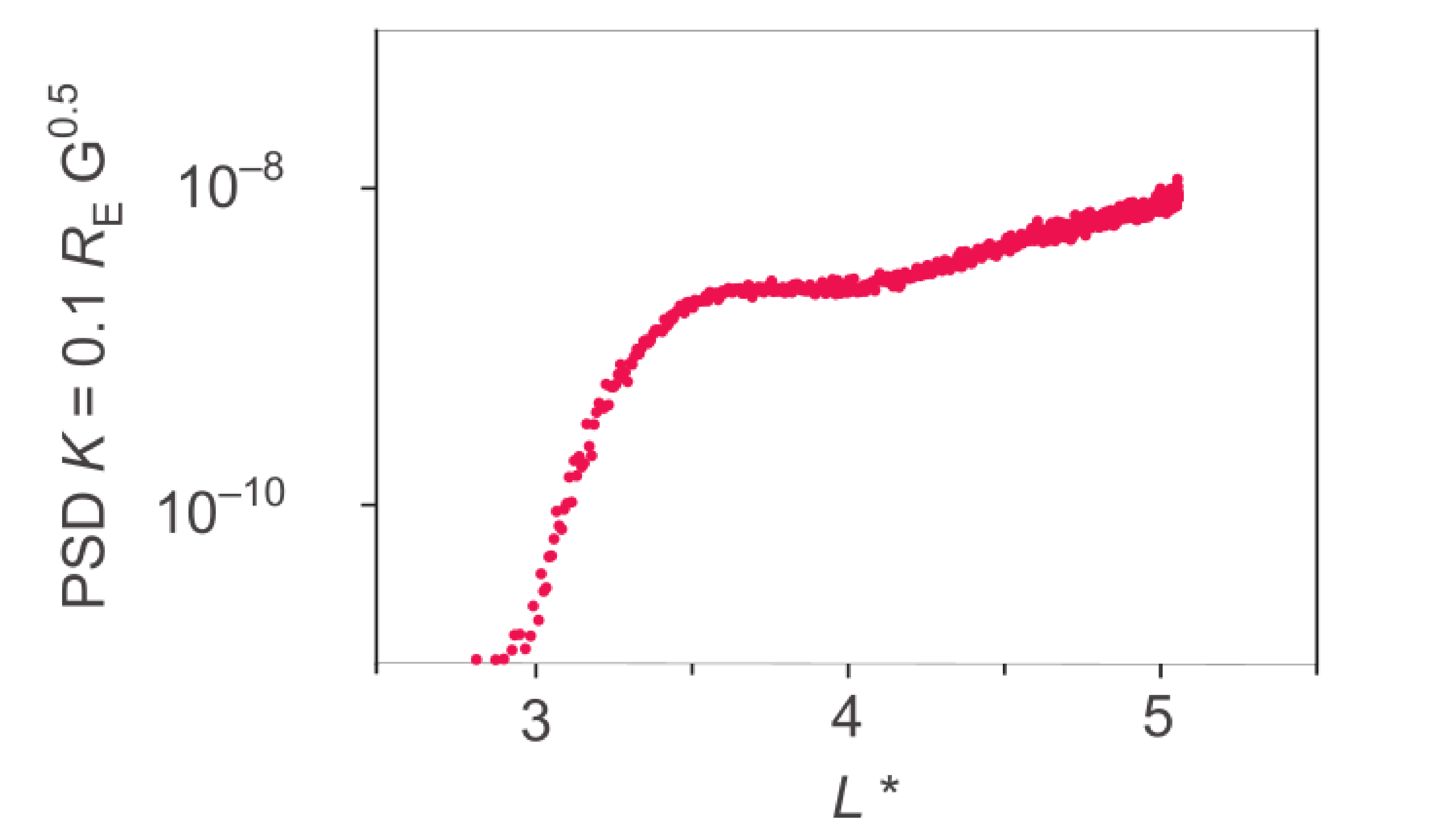

Mann et al. (2018)
K = 0.1

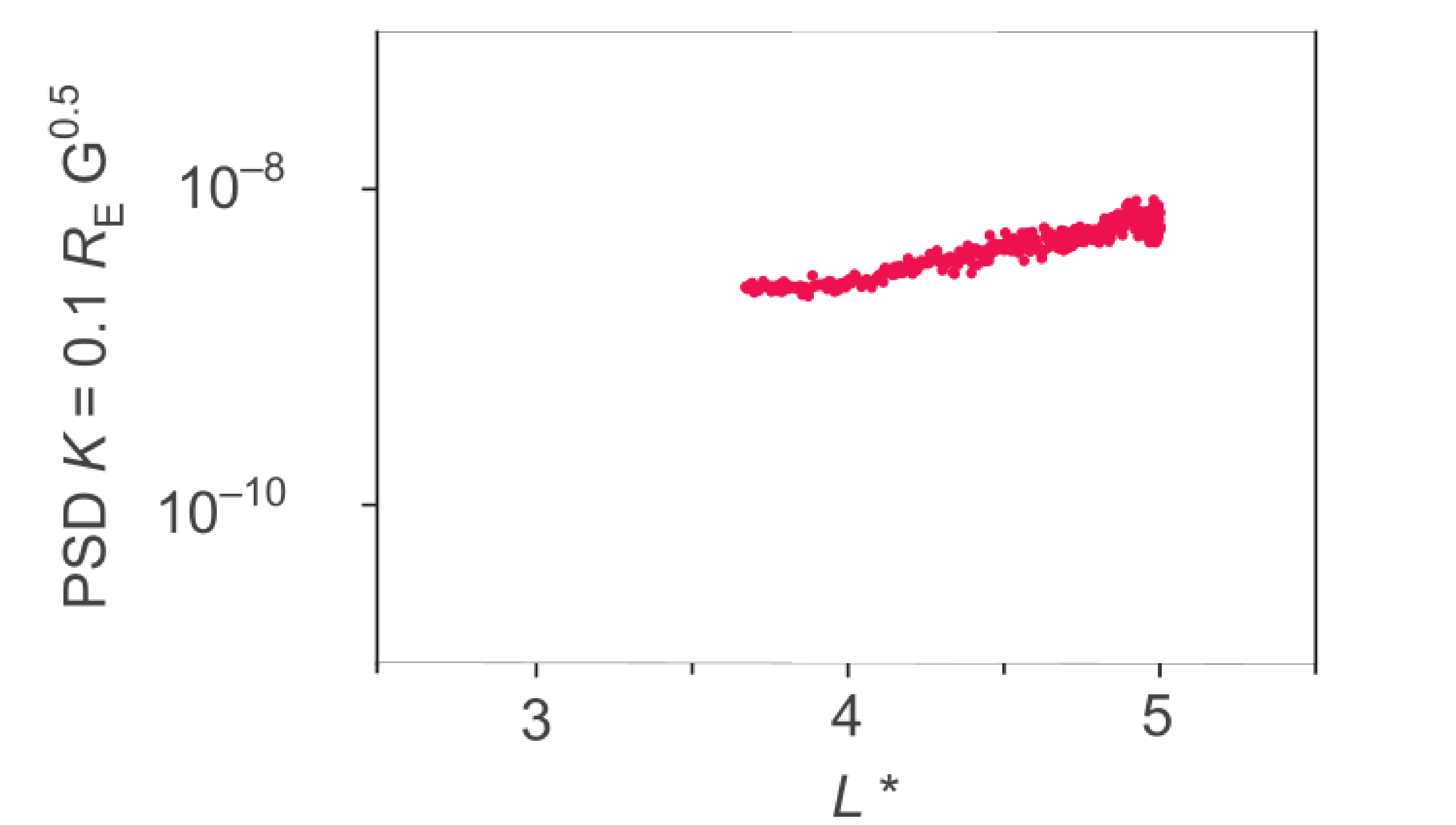

Mann et al. (2018)
K = 0.1

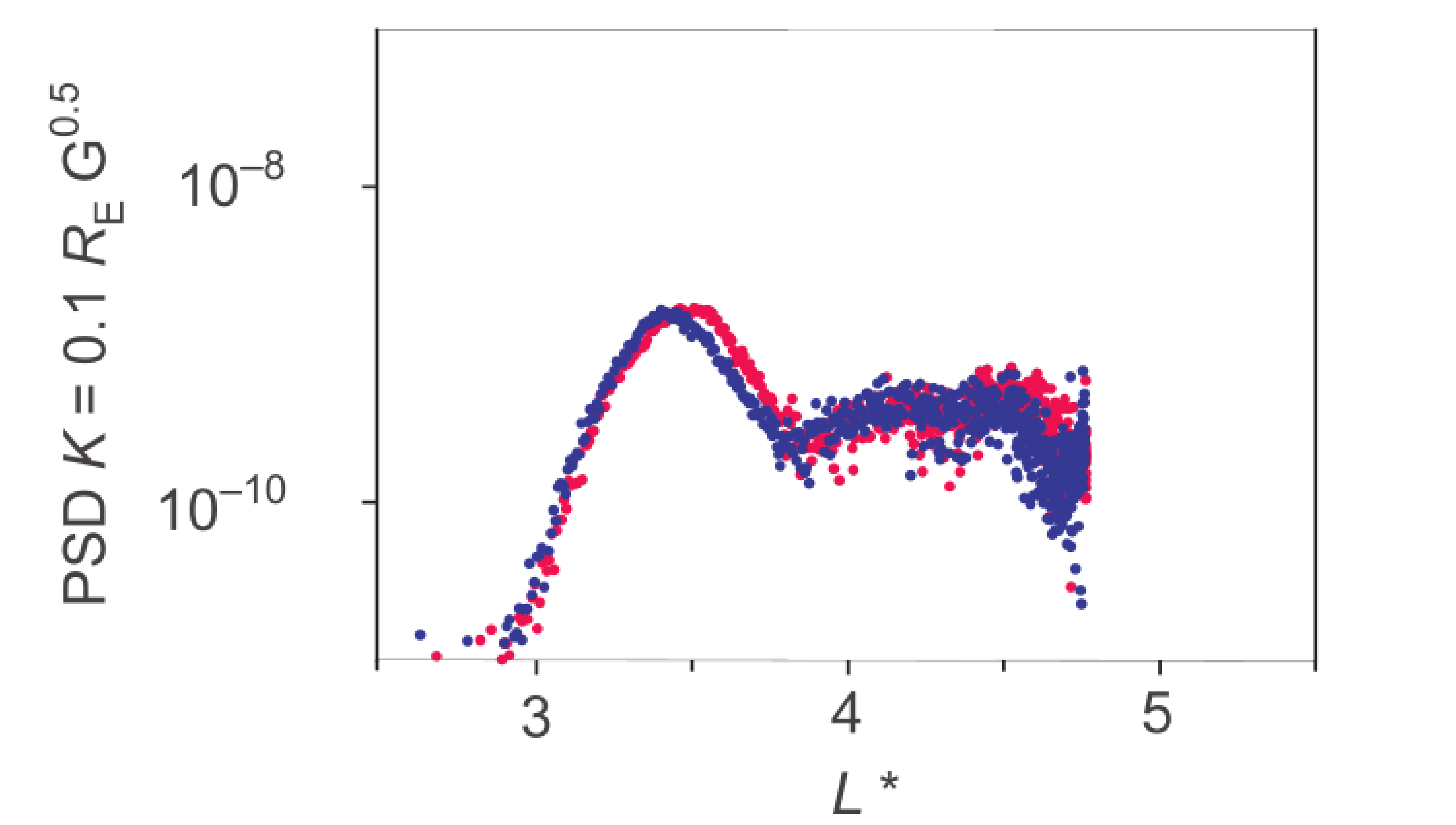

Mann et al. (2018)
K = 0.1

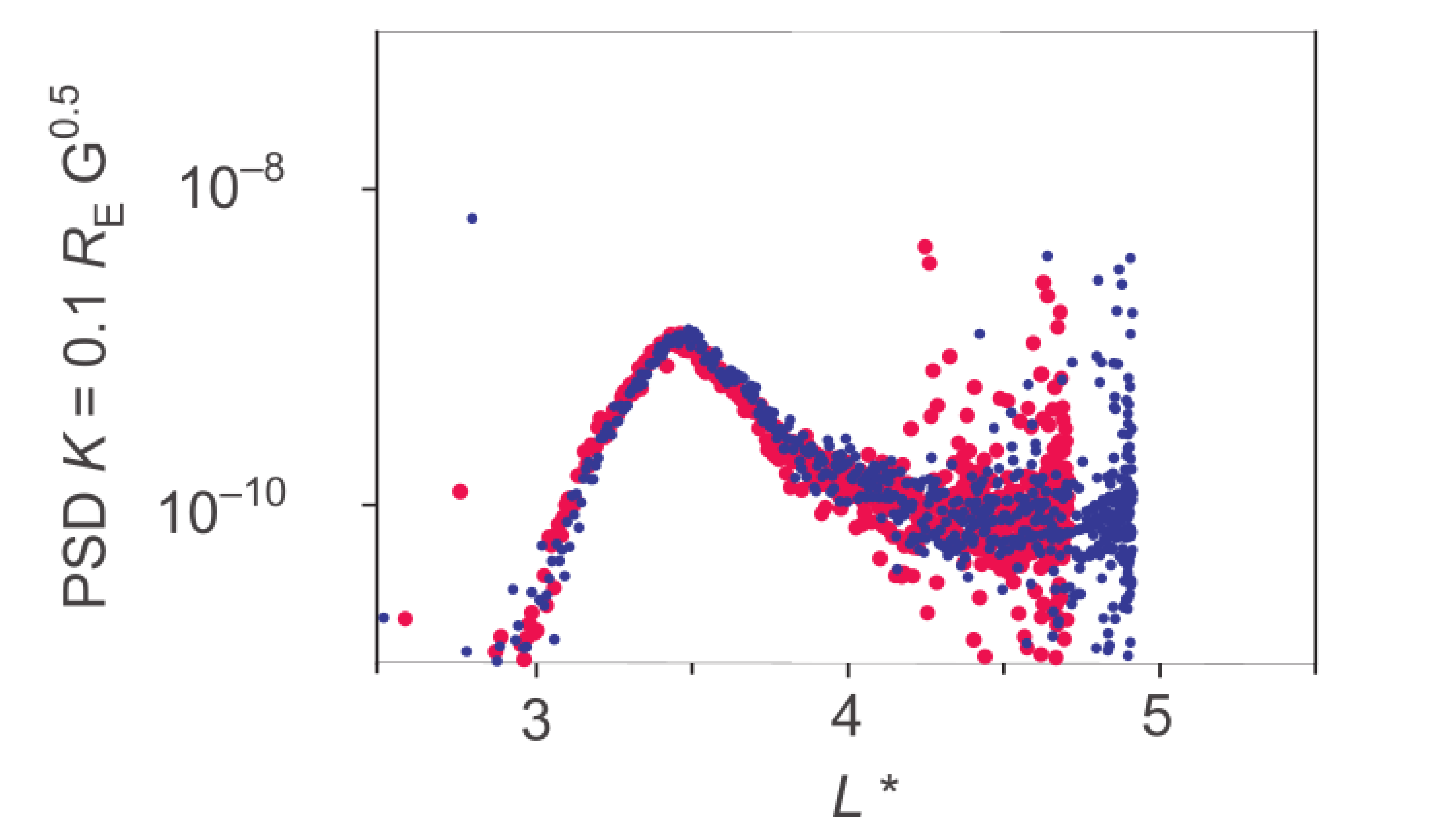

Mann et al. (2018)
K = 0.1

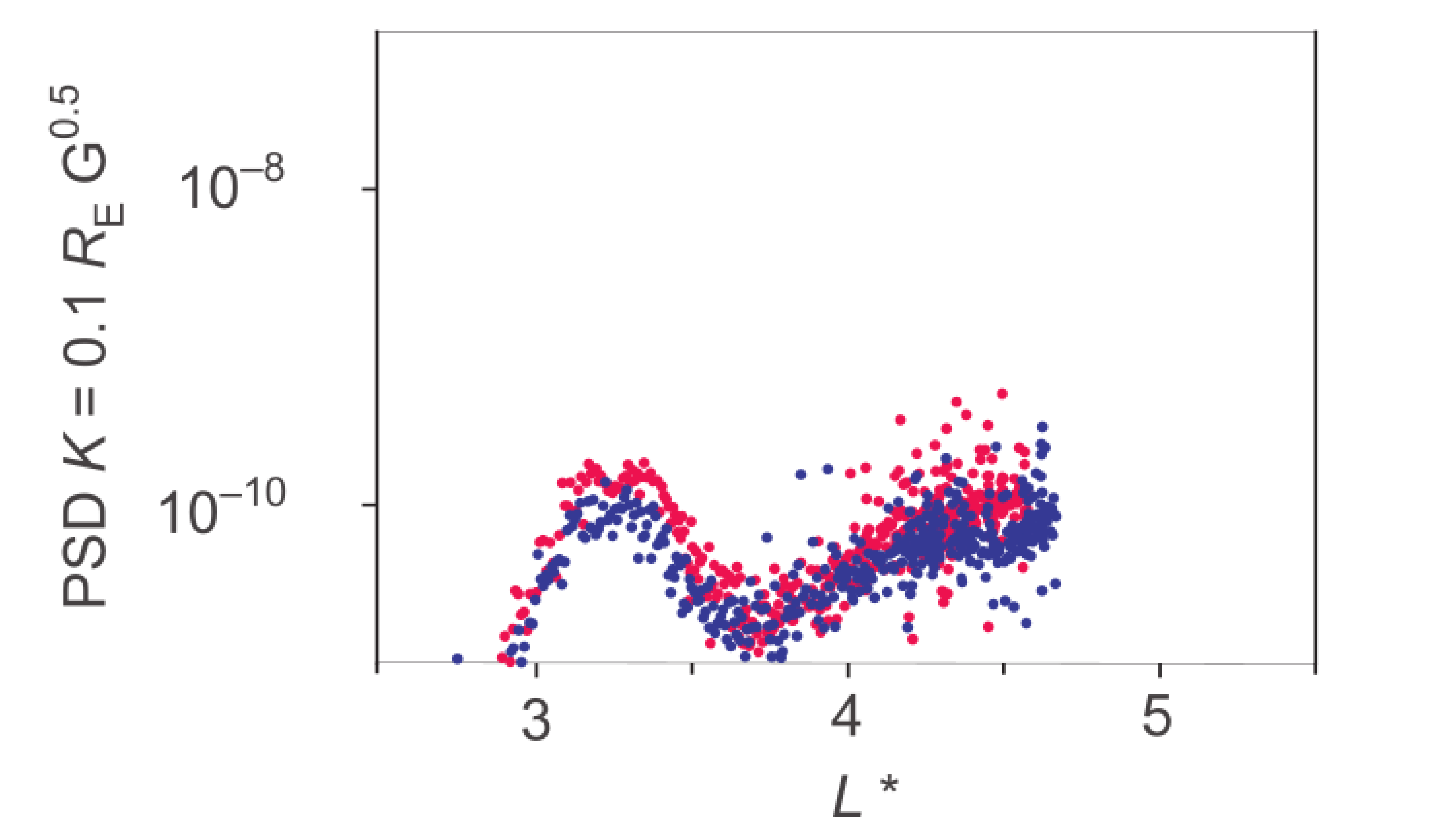

Mann et al. (2018)
K = 0.1

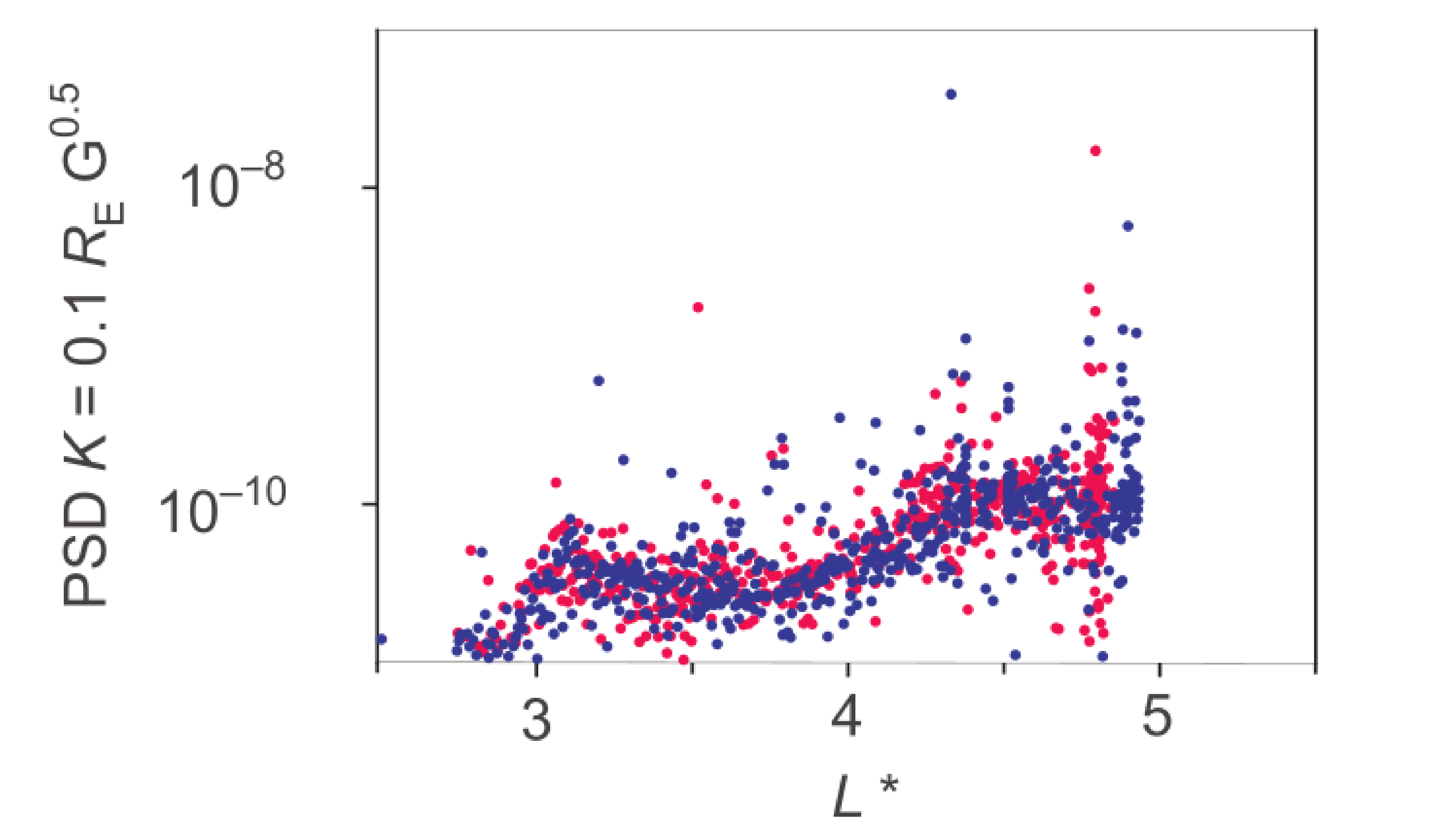

Mann et al. (2018)
K = 0.1

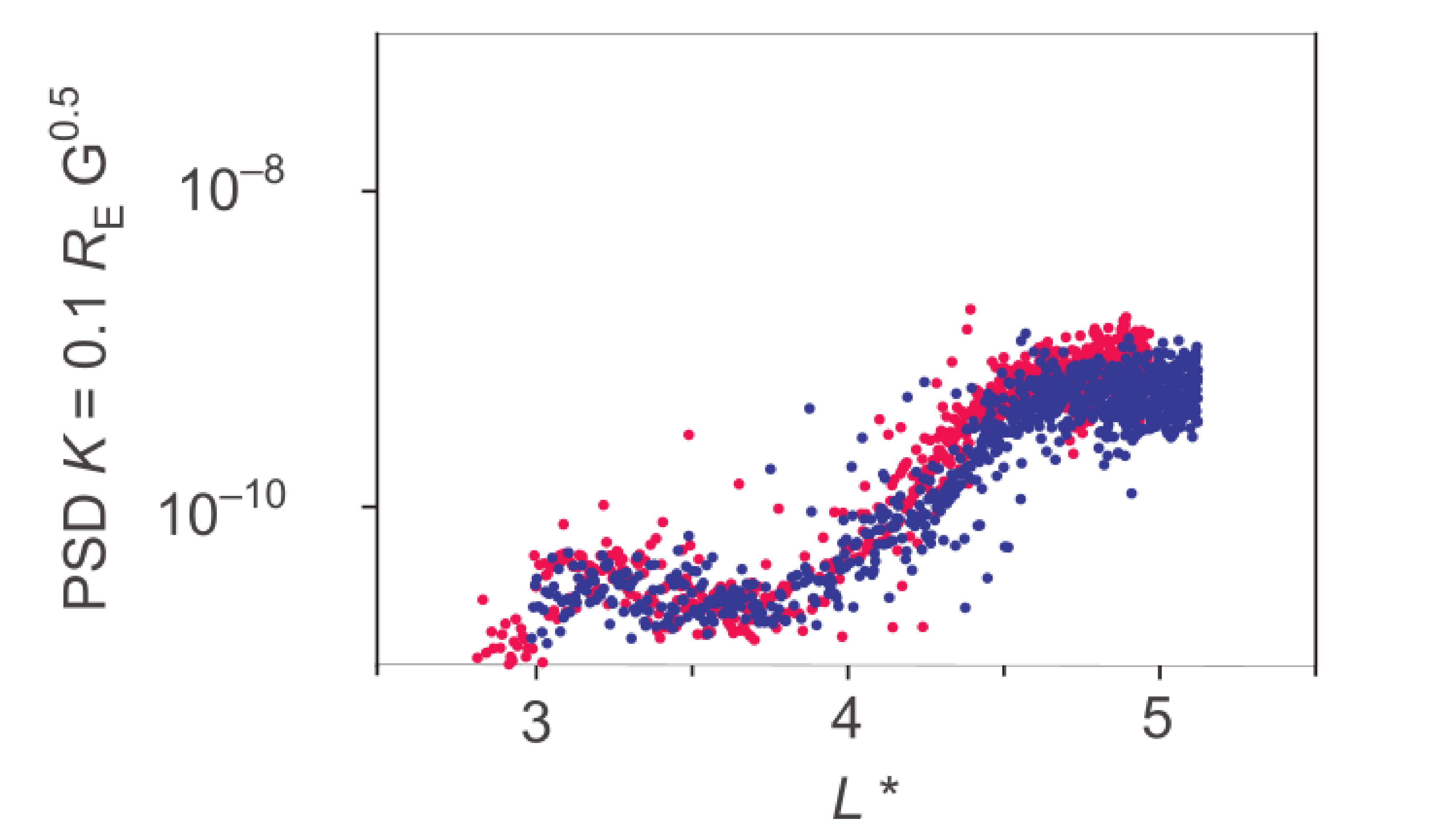

Mann et al. (2018)
K = 0.1

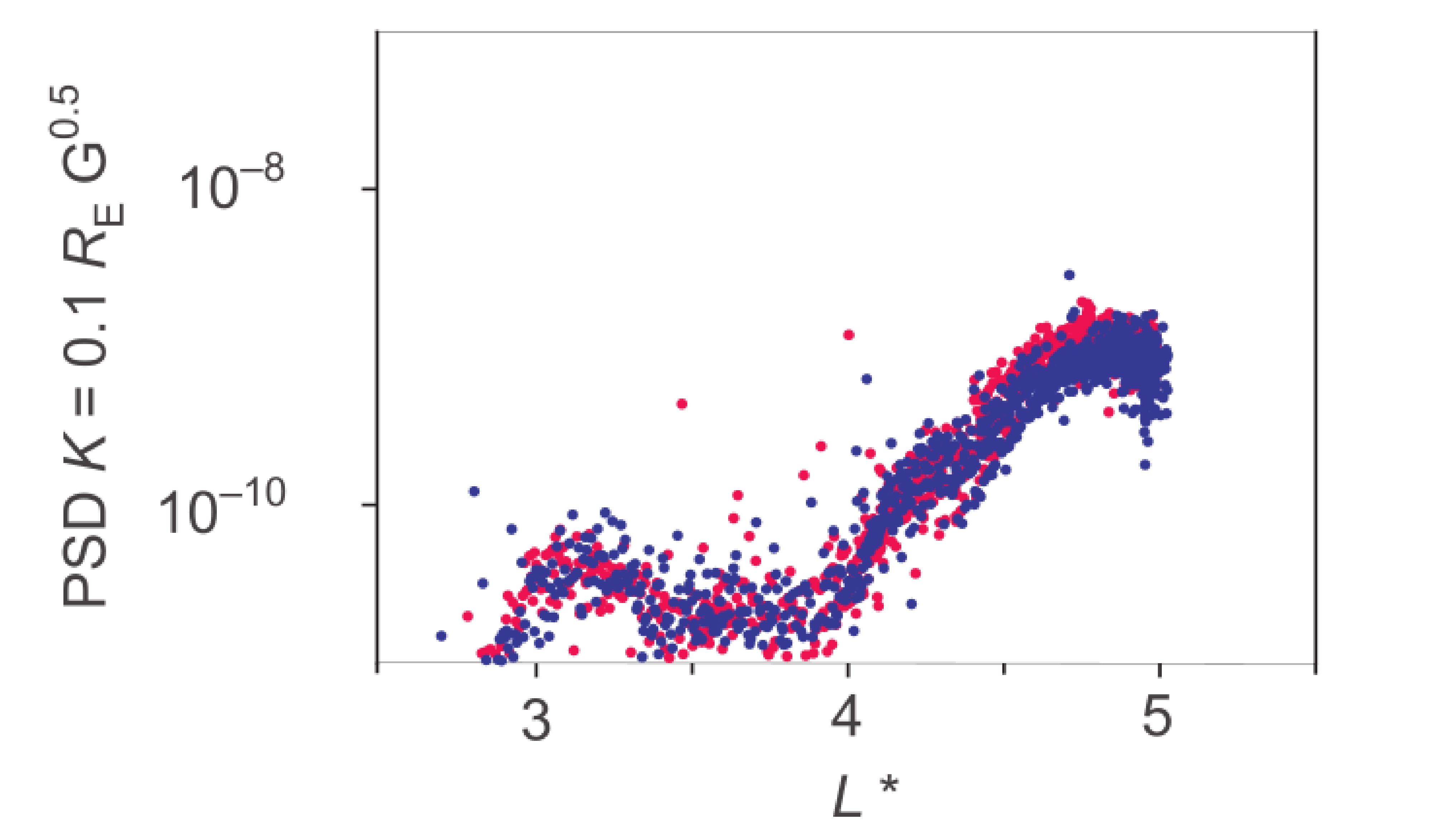

Comparison of the Evolutions of the Modeled and Observed Radial Profiles of Fluxes

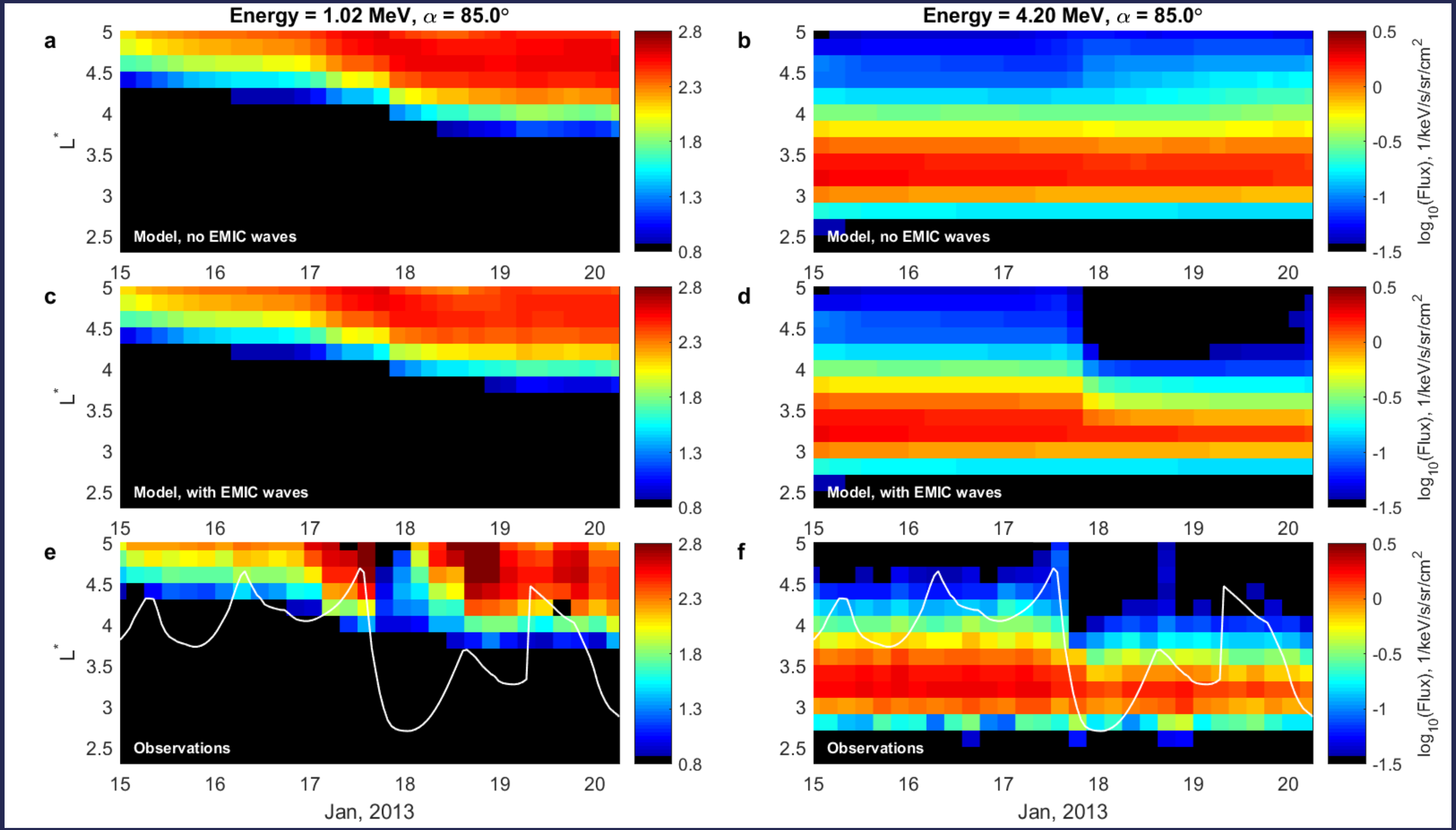

[Shprits et al., 2016, Nature Comms.]

Evolution of the Pitch Angle Distribution

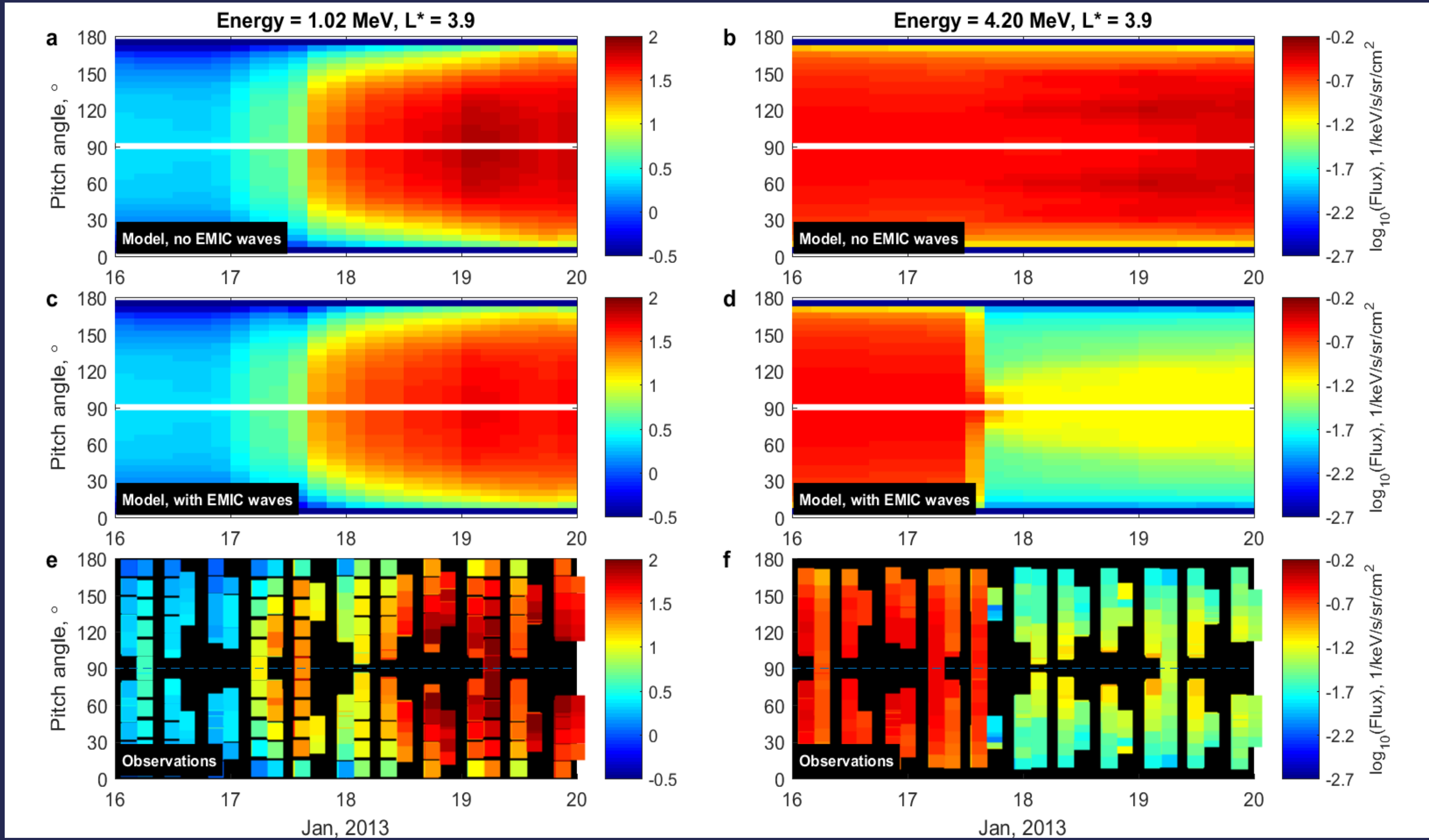

[Shprits et al., 2016, Nature Comms.]

Simulations with and without EMIC waves

Observations

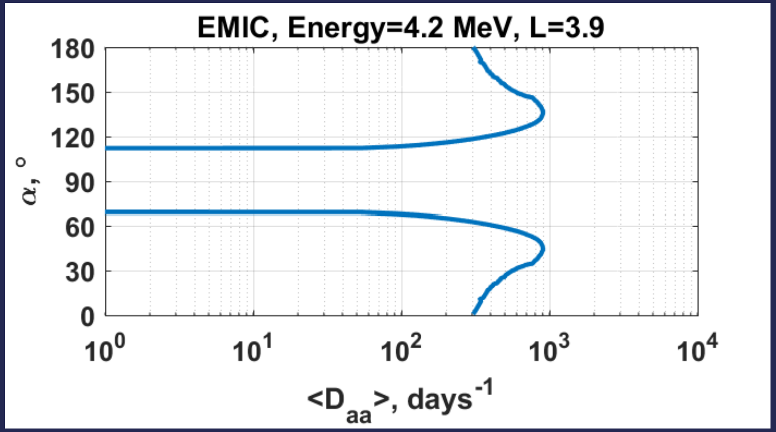

Model without EMIC

EMIC waves pitch angle diffusion coefficient

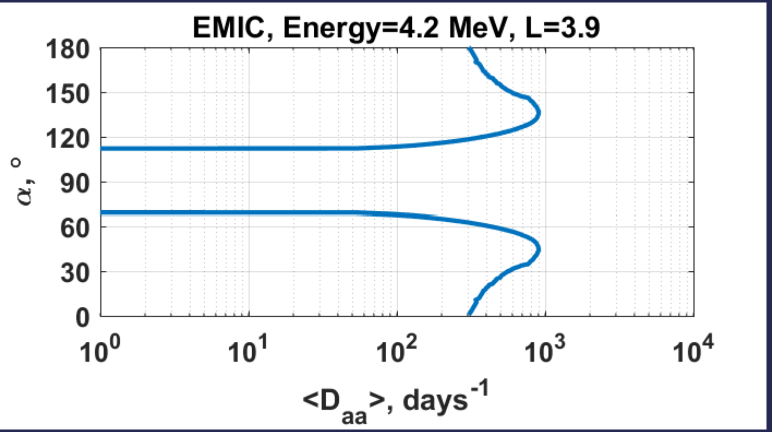

Model with EMIC

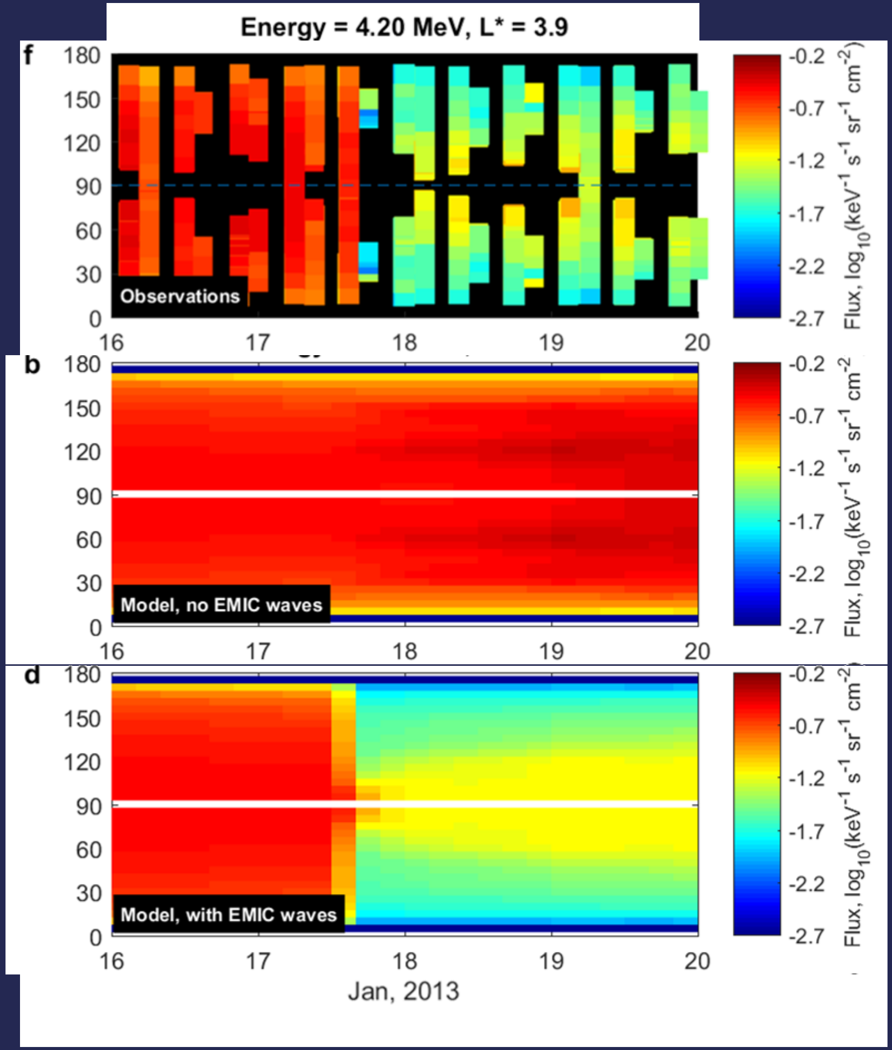

[Shprits et al., 2016, *Nature Comms.*]

Difference in Behavior of Ultra-relativistic and Relativistic Electron Fluxes

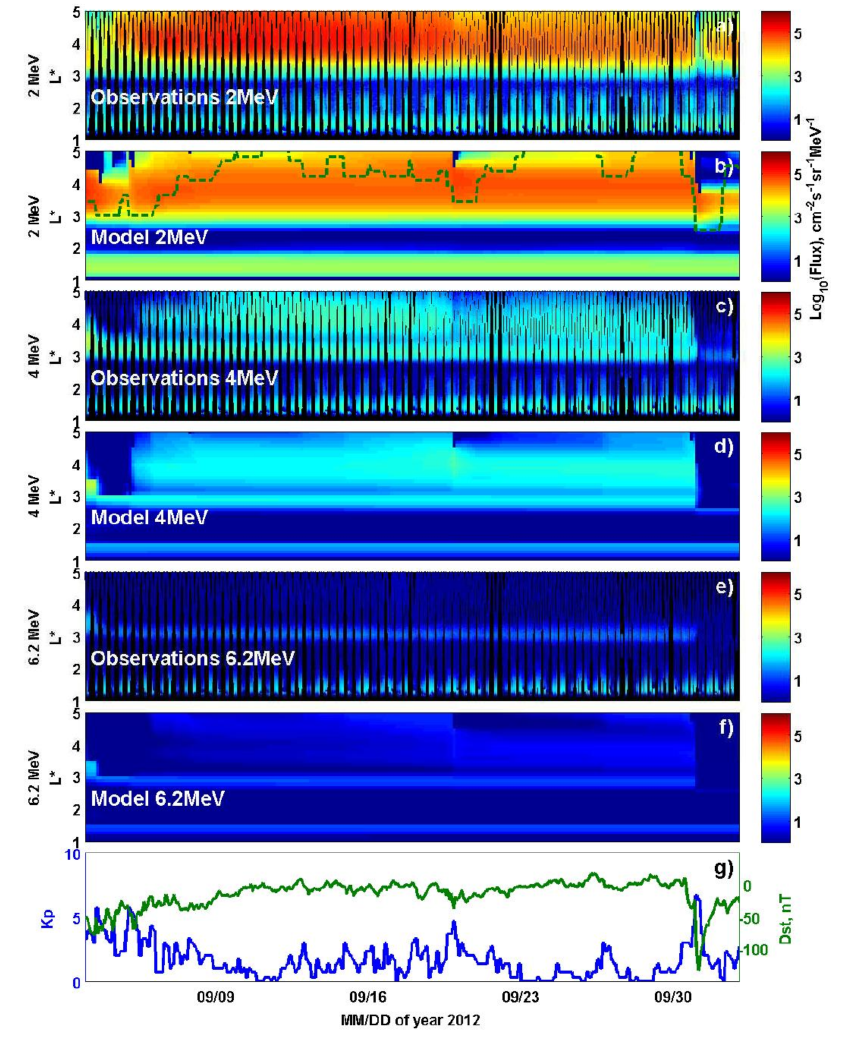

[Shprits et al., 2013, *Nature Physics*]

- Simulations with EMIC wave scattering can reproduce unusual behavior of the radiation belts.
- Simulations with EMIC scattering reproduces 3 zone structure at 4MeV and a very narrow remnant belt at 6.2 MeV.
- Simulations without EMIC waves can not reproduce such narrow remnant belts.

Analysis of PSD Profiles Presented by Mann et al. (2016)

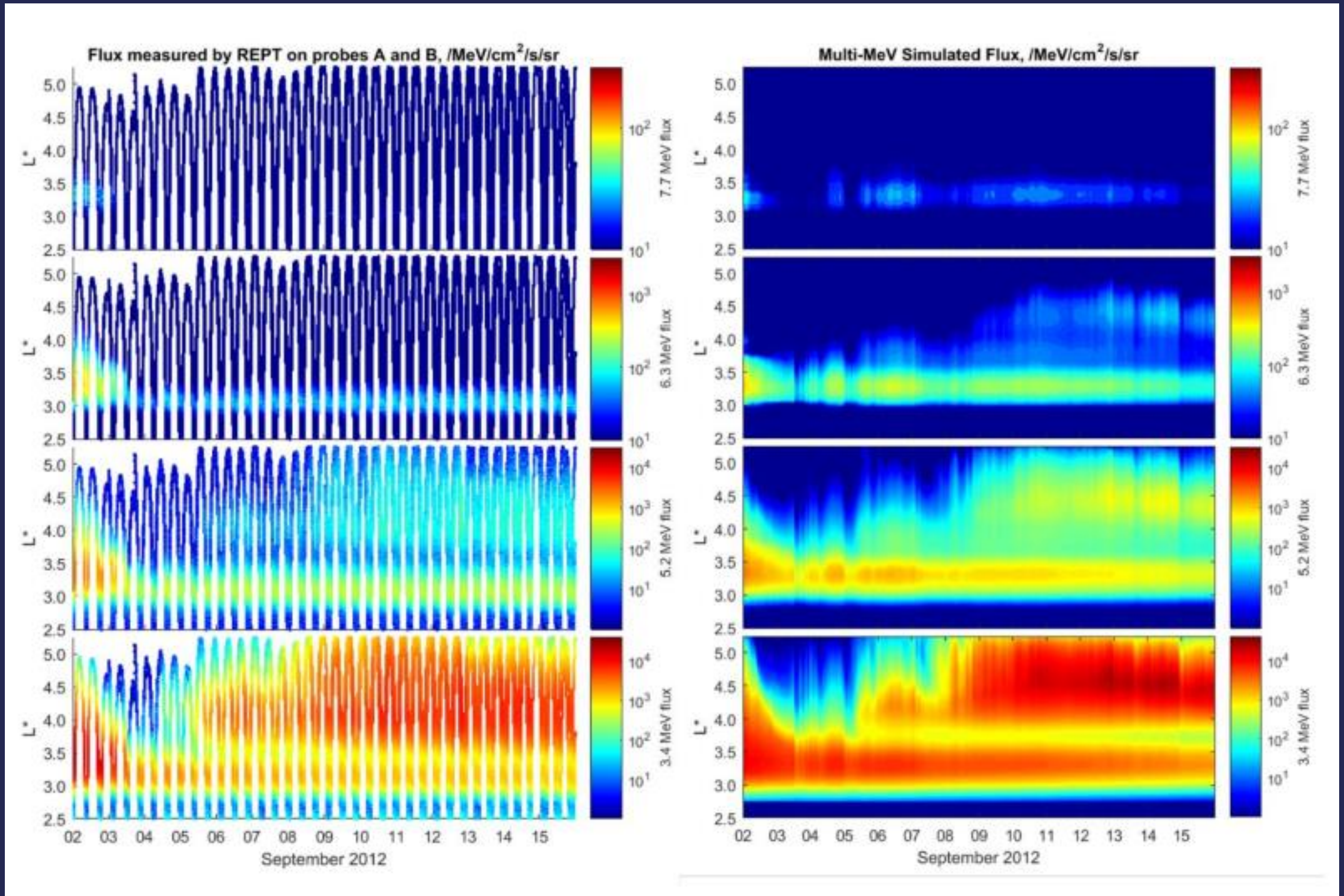

[Mann et al., 2016, *Nature Physics*]

Narrow remnant belt

Simulations of loss to MP and 3 diffusive processes

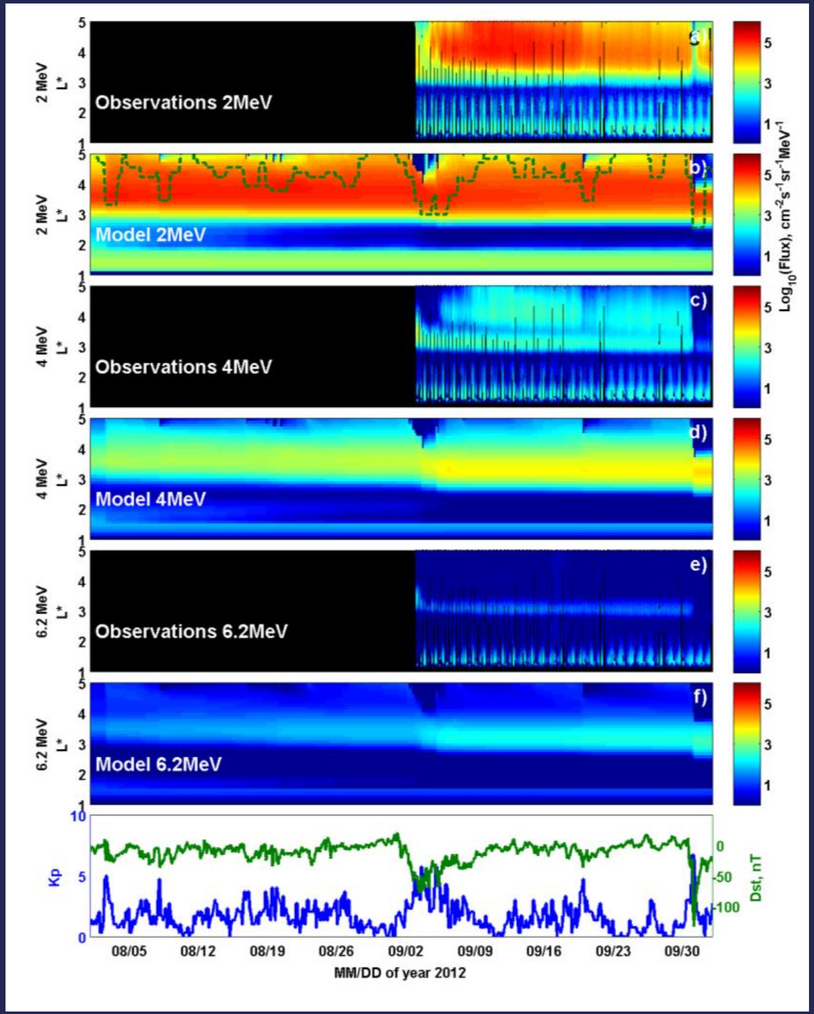

[Shprits et al., 2013 *Nature Physics*]

- Magnetopause loss that can explain for the loss of particles at relativistic energies cannot explain losses at ultra-relativistic energies.
- Additional loss process is required to produce a narrow ring of radiation.

Density: $\mu + 1\sigma$ Sheeley model Sheeley model for *αeq=30°*

H Band	A = 0.5	A = 1.0	A = 1.5
Ratio 1	4.60 / 6.93 / 8.07	1.50 / 2.38 / 2.81	0.98 / 1.59 / 1.90
Ratio 2	Nan / Nan / Nan	3.04 / 4.63 / 5.42	1.53 / 2.42 / 2.86
Ratio 3	Nan / Nan / Nan	1.70 / 2.66 / 3.14	1.03 / 1.68 / 2.00
Ratio 4	Nan / Nan / Nan	3.84 / 5.81 / 6.78	1.69 / 2.66 / 3.13
He Band	A = 0.5	A = 1.0	A = 1.5
Ratio 1	2.06 / 2.82 / 3.32	1.76 / 2.48 / 2.93	1.61 / 2.27 / 2.69
Ratio 2	2.91 / 3.77 / 4.43	2.45 / 3.26 / 3.84	2.15 / 2.94 / 3.46
Ratio 3	1.74 / 2.34 / 2.77	1.51 / 2.10 / 2.49	1.38 / 1.96 / 2.33
Ratio 4	2.26 / 2.95 / 3.48	1.94 / 2.60 / 3.07	1.77 / 2.44 / 2.88

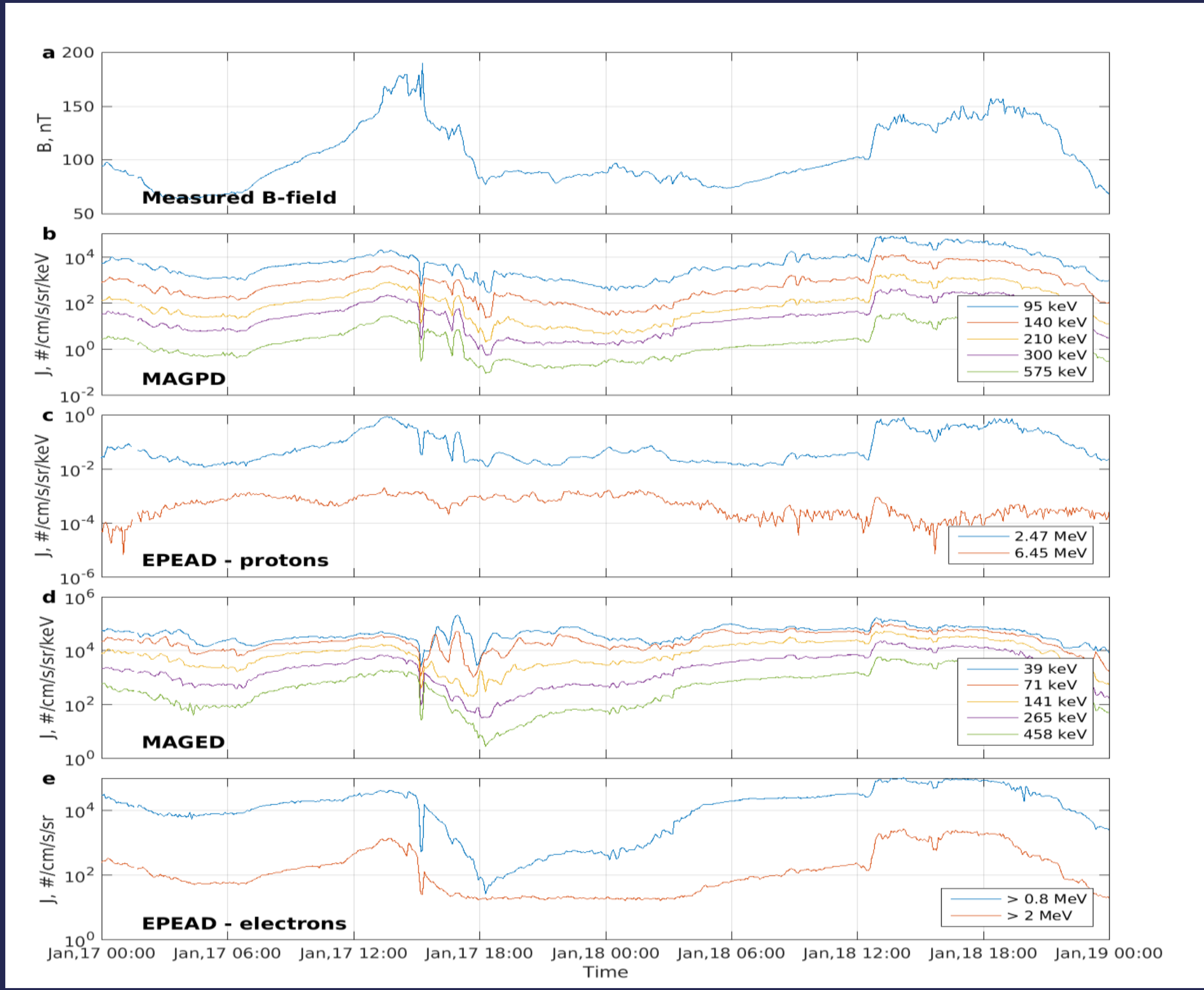

a
B, nT
Measured B-field
b
J, #/cm/s/sr/keV
MAGPD
95 keV
140 keV
210 keV
300 keV
575 keV
c
J, #/cm/s/sr/keV
EPEAD - protons
2.47 MeV
6.45 MeV
d
J, #/cm/s/sr/keV
MAGED
39 keV
71 keV
141 keV
265 keV
458 keV
e
J, #/cm/s/sr
EPEAD - electrons
> 0.8 MeV
> 2 MeV
Jan,17 00:00
Jan,17 06:00
Jan,17 12:00
Jan,17 18:00
Jan,18 00:00
Jan,18 06:00
Jan,18 12:00
Jan,18 18:00
Jan,19 00:00
Time

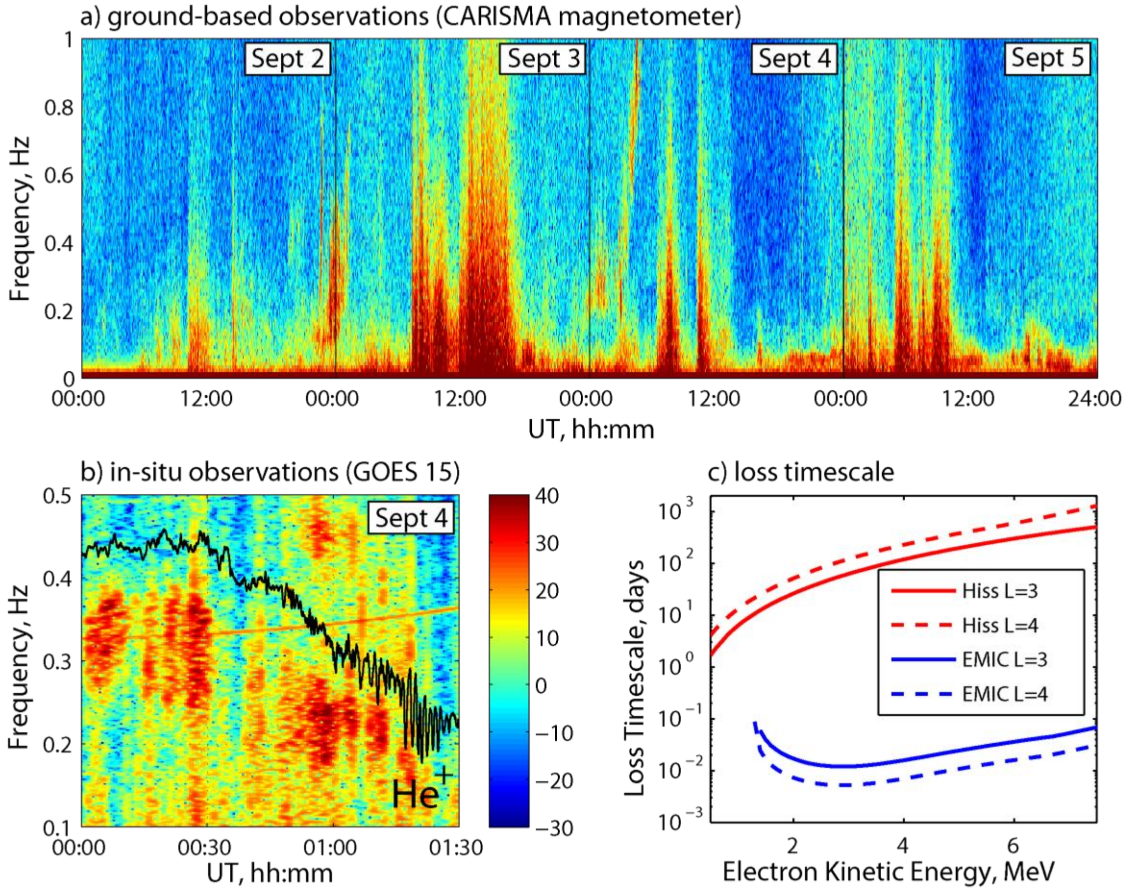

a) ground-based observations (CARISMA magnetometer)
Sept 2
Sept 3
Sept 4
Sept 5
Frequency, Hz
UT, hh:mm
b) in-situ observations (GOES 15)
Sept 4
He+
Frequency, Hz
UT, hh:mm
c) loss timescale
Hiss L=3
Hiss L=4
EMIC L=3
EMIC L=4
Loss Timescale, days
Electron Kinetic Energy, MeV